Environmental Science and Pollution Research (2020) 27:12967–12994
https://doi.org/10.1007/s11356-020-08096-6

REVIEW ARTICLE

Processing and modification of hydrogel and its application in emerging contaminant adsorption and in catalyst immobilization: a review

Hongxue Du[1,2] · Shuyun Shi[1,2] · Wei Liu[1,2] · Honghui Teng[1,2] · Mingyue Piao[1,2]

Received: 3 October 2019 / Accepted: 12 February 2020 / Published online: 2 March 2020

Abstract

Due to the wonderful property of hydrogels, they can provide a platform for a wide range of applications. Recently, there is a growing research interest in the development of potential hydrogel adsorbents in wastewater treatment due to their adsorption ability toward aqueous pollutants. It is important to prepare such a hydrogel that possesses appropriate robustness, adsorption capacity, and adsorption efficiency to meet the need of water treatment. In order to improve the property of hydrogels, much effort has been made by researchers to modify hydrogels, among which incorporating inorganic components into the polymeric networks is the most common method, which can reduce the product cost and simplify the preparation procedure. Not only can hydrogel be applied as adsorbent, but it also can be used as matrix for catalyst immobilization. In this review, the key advancement on the preparation and modification of hydrogels is discussed, with special emphasis on the introduction of inorganic materials into polymeric networks and consequential changes in the properties of mechanical strength, swelling, and adsorption. Besides, hydrogels used as adsorbents for removal of dyes and inorganic pollutants have been widely explored, but their use for adsorbing emerging contaminants from aqueous solution has not received much attention. Thus, this review is mainly focused on hydrogels' application in removing emerging contaminants by adsorption. Furthermore, hydrogels can be also applied in immobilizing catalysts, such as enzyme and photocatalyst, to remove pollutants completely and avoid secondary pollution, so their progress as catalyst matrix is overviewed.

Keywords Emerging contaminant adsorption · Hydrogel carrier · Hydrogel composites · Hydrogel modification

Introduction

Hydrogels are 3D-structured networks which can be polymerized by physical or chemical crosslinking using water-soluble polymers or monomers as gel solution. In a standard approach, the polymerization reaction is initiated by external stimuli, such as thermal, chemical activation, or irradiation, through initiators and/or catalysts. Hydrogels' unique characteristics, such as desired functionality, reversibility, and biocompatibility, meet both material and biological requirements; thus, they are commonly used for tissue regeneration, cell-laden, drug release, biosensor, and so on (Jiang et al. 2019; Mahinroosta et al. 2018; Ullah et al. 2015). Also, they can be used to improve electrical conductivity (Lin et al. 2019a), release agrochemicals (Chen and Chen 2019), and reserve water in soil (Gholamhoseini et al. 2018). In recent years, there has been a growing interest in the application of hydrogel adsorbents in pollution control due to their super adsorption capacity.

As is known to all, emerging contaminants (ECs) have raised global concern for their significant threat to aquatic ecosystem and human health. Many ECs have no regulatory standards due to the lack of information on the effects of chronic exposure. Pharmaceuticals and endocrine-disrupting chemicals are some of the most frequently detected ECs in aquatic environments (Tran et al. 2018). Conventional wastewater treatment processes are not currently designed to sufficiently treat and remove ECs from the influent, with the

Responsible editor: Tito Roberto Cadaval Jr

✉ Mingyue Piao
2577246959@qq.com

[1] Key Laboratory of Environmental Materials and Pollution Control, the Education Department of Jilin Province, Jilin Normal University, Siping, China

[2] College of Environmental Science and Engineering, Jilin Normal University, 1301 Haifeng Road, Siping 136000, China

remaining pollutants entering the environment inevitably (Wang et al. 2019b; Zhao et al. 2018a). These contaminants can accumulate and thus cause adverse effects on ecosystems (USEPA 2019, accessed Sep 2019; Zhao et al. 2018a) because they are stable under various conditions such as aerobic digestion, light, and heat. Therefore, adsorption technology has been extensively adopted to treat ECs as it is cost-effective and highly efficient.

Among various adsorbents (Elgarahy et al. 2019; Hai 2016; Kiruba et al. 2014; Neeraj et al. 2016; Senthil Kumar et al. 2018), hydrogel adsorbents show super high adsorption capacity, fast adsorption efficiency, and wide pH independence; thus, they can be chosen as an alternative for ECs' elimination. However, the poor mechanical strength of hydrogels limits their application in the elimination of pollutants because of the harsh environment during the water treatment process; therefore, it is imperative to develop suitable reinforcing agents or fillers into hydrogel networks to improve their mechanical strength (Alam et al. 2018; Zhao et al. 2015). Some inorganic materials can not only be utilized as fillers to improve physical and chemical properties of hydrogels (Afzal et al. 2018; da Silva et al. 2018; Kang et al. 2019; Rao et al. 2019; Rotbaum et al. 2019; Tong et al. 2019; Yu et al. 2018a), but also satisfy specific roles, for example, the incorporation of TiO_2 can provide the hydrogel with photocatalytic properties (Yu et al. 2018b), and Fe_3O_4 (Liang et al. 2019b; Meng et al. 2019; Tang et al. 2014; Zhang et al. 2019b) and Fe_2O_3 (Badsha and Lo 2019; Khan and Lo 2017) can afford the hydrogel with magnetic separation and oxidant properties.

A host of review papers is dedicated to the application of hydrogel in adsorption of dyes, metals, and some other inorganic substances (Khan and Lo 2016; Van Tran et al. 2018; Zheng and Wang 2015), but to our knowledge, using hydrogel adsorbents to remove ECs has not been extensively reviewed. Furthermore, while the adsorption property of hydrogels has been commonly investigated, their sustainable regeneration methods are not developed sufficiently. As is known to all, a suitable regeneration method is a major challenge for low-cost and long-term running. Hydrogels have the potential as carriers for catalyst immobilization in order to eliminate pollutants completely for reuse purpose, but that has not received much attention until now. This review aims to provide a coverage of the latest developments in the modification of hydrogels, especially by inorganic fillers, and consequently, their changes in mechanical strength, swelling ratio, and adsorption property. Furthermore, hydrogels as adsorbents for removing ECs and as carriers for immobilizing catalysts are reviewed.

Throughout this article, the name of a hydrogel will be based on its monomer (or polymer)/monomer (or polymer)-filler. For example, a hydrogel composite consisting of alginate sodium (SA), hyaluronic acid (HA), and Fe_2O_3 will be mentioned as SA/HA–Fe_2O_3.

Preparation of hydrogel

Hydrogels can be synthesized using natural, synthetic, and/or blend of natural/synthetic materials. The free radical polymerization is the most widely used method to prepare hydrogels (Qi et al. 2019a; Shariatinia and Jalali 2018; Ullah et al. 2015). In a typical hydrogel formulation, the gel precursor reacts with crosslinker(s) to form 3D-crosslinked networks. Examples of some commonly used crosslinking agents include potassium persulfate or ammonium persulfate (Khan and Lo 2016). As shown in Fig. 1, free radical polymerization comprises three main stages: initiation, propagation, and termination (Khan and Lo 2016). In the initiation stage, free radicals ($R^{\bullet}$) are generated by the dissociation of an initiator. The polymerization reaction is usually initiated using thermal stimulus (Zhuang et al. 2019). Besides, irradiation, e.g., γ-ray or ultraviolet ray, has recently attracted much attention, because it allows rapid conversion of gel solution to solid hydrogel under physiological condition (Aycan and Alemdar 2018; Du and Piao 2018; Sun et al. 2019b). Also, the combination of the two methods is feasible (Yu et al. 2018b). The free radicals then react with molecules of monomer (or polymer) (M) to produce the first radicals $M^{\bullet}$. Due to the very high reactivity of free radicals, they instantly react on molecules of monomer (or polymer), leading to growth of macroradicals (propagation stage). Termination usually takes place by combination or disproportionation reaction. Various shape of hydrogels, such as bulk (Song et al. 2019), sphere (Liu and Garcia 2016; Mohammadian et al. 2019; Wang et al. 2018b), and film (Getachew et al. 2019; Sun et al. 2019b) can be designed by choosing the appropriate preparation method, raw material, and polymerization condition.

Preparation of bulk hydrogels

Generally, bulk hydrogel can be easily obtained by solution polymerization. It is a homogeneous polymerization in which all the constituents including the monomer (or polymer), initiator, and crosslinking agent are soluble in the medium. The synthesized bulk hydrogel usually takes the shape of the container in which it is polymerized (Qi et al. 2019a). Song et al.

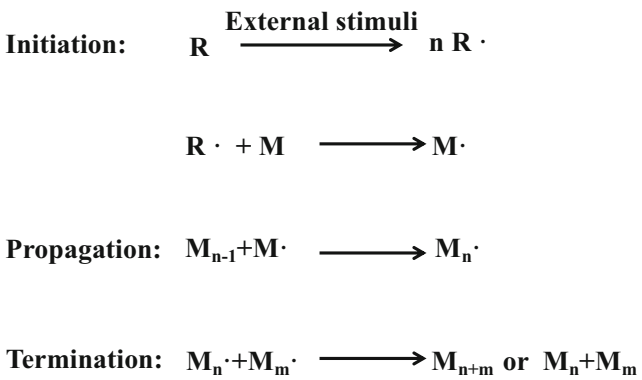

Fig. 1 Free radical polymerization process

stirred the mixture of 5% carboxymethyl cellulose (CMC) and 4% polyethylenimine (PEI) solution added with 2% crosslinking agent epichlorohydrin (ECH) before pouring them into a closed tube, and placed in a constant temperature drying oven at 60 °C for 4 h to obtain white cylindrical CMC/PEI hydrogel, then it was directly used for removing Cr(VI) (Song et al. 2019). Qi et al. prepared salecan hydrogel for removal of Cu(II). They first mixed all the solution, including 2% salecan, crosslinking agent, and initiator, and then poured them into a Teflon mold and kept at 70 °C for 6 h to facilitate the polymerized reaction (Qi et al. 2019b).

This approach can yield a relatively homogeneous hydrogel. However, long equilibrium time is often reported during water treatment (Tang et al. 2010), due to the slow diffusion transport of pollutant to the adsorption sites within hydrogel networks. Thus, for better mass transfer efficiency, bulk hydrogel is often cut into a small-sized pieces manually (Shah et al. 2018) or is transferred to a food blender to produce hydrogel beads having a much smaller size than bulk shape (Thompson et al. 2018). However, the cutting or grinding step has the possibility to yield hydrogel particles with polydispersity and damaged morphology. So, spherical hydrogel is an alternative because grinding or cutting is not required and thus avoids further energy consumption and morphology destruction.

Preparation of spherical hydrogels

Hydrogel bead is one type of spherical hydrogel with a millimeter diameter. It is generally synthesized by dropping the monomer (or polymer) suspension solution into a hardened solution by a syringe; thus, the size of the hydrogel bead is usually dependent on the diameter of the syringe. SA is the most commonly used material for the synthesis of hydrogel bead (Thakur et al. 2018). The interest in the preparation of SA hydrogel comes from its ionic characteristics. It has carboxylic groups along its chains, which can be converted to ionized form, generating electrostatic anion–anion repulsion forces that make it easier for the polymeric chains to expand in water. SA precursor forms to 3D-crosslinked hydrogel networks by contacting with hardened solution of cations, such as Ca(II) (Ohemeng-Boahen et al. 2019; Pathak et al. 2016; Wang et al. 2019a; Yang et al. 2018b; Zhao et al. 2018b) and Ag(I) (Lengert et al. 2019). During the gelation process, the hardened cations bind to two carboxyl groups on the adjacent alginate molecules which can be explained by the egg-box model. Chitosan (CS), a biodegradable, biocompatible, odorless, and nontoxic biopolymer, is another commonly used natural polysaccharide for hydrogel bead preparation. Similarly, CS can be crosslinked by contacting with cations, such as Na ion (Afzal et al. 2019; Ahmad et al. 2019; Kluczka et al. 2018; Ren et al. 2019) and K ion (Bilal et al. 2019a). Other materials are also used for hydrogel bead synthesis. Benhalima et al. mixed the solution of CMC and dextran sulfate, and then dropped the mixture into Al(III) solution to prepare hydrogel bead (Benhalima and Ferfera-Harrar 2019). Polyacrylic acid (PAA) hydrogel bead was obtained by dropping the precursor solution into polyethersulfone/N,N-dimethylformamide (PES/DMF) using a syringe needle with 0.7 mm in diameter, and then applied to remove dyes of MB and MO (Yang et al. 2019a). Boric acid (Mohammadian et al. 2019) and liquid nitrogen (Yu et al. 2015) can also be used as hardening agent to make hydrogel bead.

Although hydrogel bead can be applied directly for pollutant adsorption process, the size is too big to transfer the pollutant effectively (Luo et al. 2019), and usually a long time is required for adsorption equilibrium. In addition to a high adsorption capacity, fast kinetic (short equilibrium time) is another desirable feature of an adsorptive treatment system from a practical viewpoint; thus, a smaller size is favored. Particle form (micro- or nano-sized) hydrogel can be synthesized directly by utilizing heterogeneous polymerization techniques (Liu and Garcia 2016); among them, a liquid–liquid two-phase system is the most common method involving polymerization in bulk solution. Different types of heterogeneous polymerizations, distinguished by the solubility of the monomer (or polymer), initiator, and resulting polymer, have been reviewed by Elbert (2011). Generally speaking, a mixing or homogenization step, by a vortex mixer or a homogenizer, is employed to generate droplets of monomer (or polymer) in one phase, surrounded by another phase (W/O or O/W). The surfactant often serves to prevent re-aggregation of the droplets in the system. After adding the initiator and adjusting the environment correctly (e.g., heating the system to a sufficient temperature for a thermal initiator), the initiator reacts to form free radicals that start the polymerization process. The polymerized product is then collected, washed, and optionally lyophilized for storage. Tuning of particle size can be achieved by applying proper methods, such as emulsion polymerization, suspension polymerization, dispersion polymerization, and precipitation polymerization. In a special method, the particle size can be further controlled by altering certain parameters such as mixing speed and reaction temperature.

The major drawbacks in liquid–liquid two-phase systems include the wide distribution of particle size and uneven distribution of specific functional groups in hydrogel networks. The microfluidic approach can solve these problems. The microfluidic synthesis scheme is continuous as opposed to batch system, and by controlling the pattern of aqueous droplets, uniform distribution of particle size and functional groups can be achieved (Dehli et al. 2019; Liu et al. 2019a; Sun et al. 2018) at the cost of a slower synthesis speed (Liu et al. 2019d). However, the application of a microfluidic device as reactor

for mass production of hydrogel is still not practical due to the complexity of the design and operation.

Preparation of hydrogel films

A film is a polymer material with selective function for separating, purifying, or concentrating different components of solution in water treatment. In practice, water filtration membrane can be damaged due to several causes, such as debris that enters the system during installation, operation, and maintenance (Goh et al. 2019). One class of membrane that seems to have a great potential for real application is hydrogel film, especially hydrogel–composite film (Raval et al. 2015; Thakur and Voicu 2016). Many hydrogels exhibit robust and repeatable self-healing in the presence of water, and they can be used as an efficient ion-exchange film for water purification (Mirabedini et al. 2016; Upama Baruah and Chowdhury 2016). Ma et al. reported a simple and fast method with low-energy consumption sunlight polymerization to directly fabricate a poly(amidoxime) hydrogel film for uranium adsorption (Ma et al. 2019).

Hydrogel film is commonly used for sensor in which it is usually employed as an active layer of membrane, primarily to render the surface of the membrane more hydrophilic and less prone to fouling (Erfkamp et al. 2019; Gogoi et al. 2015; Yin and Ma 2019). Wu et al. designed and fabricated a visual volumetric sensor platform with fluorescein-crosslinked polyacrylamide (PAM) hydrogel. The sensor underwent volumetric response to S^{2-}, enabling its visual quantitative detection (Wu et al. 2019b). Nam et al. described a colorimetric hydrogel biosensor for rapid detecting nitrite ions using polyethylene glycol (PEG) hydrogel superimposed glass fiber membrane strips (Nam et al. 2018). Kishore et al. investigated a stimulus-responsive hydrogel encompassed with tetraalkylammonium salts which was specifically sensitive to Cr(VI) (Kishore et al. 2017). For detection of Fe(II), Martínez et al. prepared a PAM hydrogel film first and then the film was immersed in ligand solution which is sensitive to Fe(II) (Martínez et al. 2017). Zhang et al. designed a carboxylated poly(*N*-isopropylacrylamide) (PNIPAAM) hydrogel and spin coated it on a gold surface by UV light irradiation for the optical sensitive detection of 17β-estradiol (E_2) (Zhang et al. 2013). Sun et al. mixed the PAM/cytochrome gel solution and coated it drop by drop on the surface of the retreated GCE for detection of bisphenol A (BPA) (Sun and Wu 2013).

It is easy to prepare hydrogel film. Usually, filtration substrate is soaked in the hydrogel precursor solution (Yin and Ma 2019), or the hydrogel precursor solution is deposited on top of the filtration substrate (Balasubramanian et al. 2018; Getachew et al. 2019; Nguyen and Liu 2014), then the coated substrate is dried (Mirabedini et al. 2016; Upama Baruah and Chowdhury 2016) or irradiated (Getachew et al. 2019; Sun et al. 2019b) to form hydrogel film. Recently, the electrospinning technique is chosen as a method to directly prepare nanofiber hydrogel film (Zhang et al. 2019a). In order to synthesize a hydrogel composite with a certain special aim, some additive can be loaded into the hydrogel film either by mixing additive with hydrogel precursor before polymerization or being grafted to the hydrogel film after polymerization (Zhang et al. 2018b).

Modification of hydrogels

Materials used for hydrogel synthesis are hydrophilic and flexible, but most of the hydrogels fracture easily, even under mild loading condition, because of their poor mechanical strength and toughness. Therefore, enhancing the strength mechanical plays a key role from a practical view. In recent years, a large effort has been done on tailoring the mechanical properties of these hydrogels to make them more suitable for various applications. Traditional methods, such as physical mixing or chemical grating, can achieve this goal at a considerable degree. Another popular method is the introduction of inorganic materials into hydrogel networks as reinforcing agents to prepare hydrogel composites, which is more effective and simple. Various modification methods are summarized in the following, with emphasis on hydrogel composites and the changes in hydrogels' properties.

Modification of hydrogels by traditional methods

During preparation of hydrogel, the mixture of more than one type of monomer (or polymer) is a commonly used method to improve the properties of hydrogel. Liu et al. found that the addition of poly(vinyl alcohol) (PVA) into hemicelluloses grafted PAA/bentonite greatly improved the mechanical strength and water absorbency (Liu et al. 2019b). Emami et al. found that increasing the oxidation of SA led to denser structure with smaller pores when SA was incorporated into gelatin hydrogel (Emami et al. 2018). Zhang et al. found that the presence of xanthan gum (XG) visibly improved the swelling ratio of PVA due to the formation of hydrogen bonds between the PVA and XG (Zhang et al. 2019c). The property of hydrogel can also be tuned by controlling the degree of crosslinking through adjusting the synthesis parameters, such as reaction temperature (Baek et al. 2018; Kim et al. 2018), gel time (Bobula et al. 2017), gel pH, crosslinking agent (Xu et al. 2017), and respective amount of different types of ingredients (Liu et al. 2018b; Pettinelli et al. 2019). But it is not sufficient to form polymeric networks if the crosslinking degree is too low, whereas too high results in compact density networks that may prevent the pollutant adsorption (Qi et al. 2018). Besides, the postprocessing technique had a strong correlation with the hydrogels' properties. Compared with air-dried hydrogels, hydrogels dried by freezing swell significantly because the

freezing process can yield micropores (Heimbuck et al. 2019). The freezing (Genevro et al. 2019) and the cyclic freeze–thaw method (Long et al. 2019) are promising and simple techniques for preparing hydrogels with improved mechanical properties.

Chemical modification is another common method to enhance hydrogels' properties. For examples, HA hydrogel post grafted with tannic acid showed improved mechanical properties compared with the pure one (Lee et al. 2018). The mechanical property, morphology, and swelling behavior of the methacrylated-carboxymethyl chitin hydrogels (Me-CMCH) could be tuned by controlling the degree of methacrylation (Kang et al. 2017). Karbarz modified the N-isopropylacrylamide (NIPAM) hydrogel with diacryloyl derivative of cystine to improve the adsorption of Cd(II) and Pb(II) (Karbarz et al. 2018). By adding sodium lignosulfonate to acrylic acid/maleic anhydride (AA/MA) hydrogel, water adsorption and Ni(II) adsorption were changed (Wang et al. 2018e). Hafezi et al. found that the adsorption of MB could be improved by adding tannic acid into pectin/dopamine hydrogel (Hafezi Moghaddam et al. 2019). CS modified by sebacoyl chloride led to a remarkable improvement in the adsorption of Hg(II), Ni(II), and Co(II) (Kandile and Mohamed 2019). Cellulose/lignin hydrogel post grafted with AA or methacryloxyethyltrimethyl ammonium chloride could increase the Cr(VI) adsorption capacity (Wang et al. 2018f).

Modification of hydrogels by inorganic fillers

Although traditional methods play an important role in modifying hydrogels, most of these methods need sophisticated control procedures. In contrast, hydrogel composites are relatively simpler to design. Compared with organic materials (Huang et al. 2018a; Jung et al. 2019; Shojaeiarani et al. 2019; Xing et al. 2019; Yue et al. 2019a), inorganic components are widely used because they are much cheaper and tougher, and often display high specific surface area, sufficient reactive sites, and fast dissolution; thus, it is a promising method that introduces inorganic materials into hydrogel networks (Wang et al. 2018a). In addition to high mechanical strength and low cost, the merit of inorganic materials is its easy preparation. Two major synthesis routes, solution mixing (Sun et al. 2019a) and impregnation (Dargahi et al. 2018; Wahid et al. 2016), have been shown schematically in Fig. 2. The first technique involves the homogeneous dispersion of inorganic materials in monomer (or polymer) solution followed by polymerization. Inorganic materials can be dispersed in most solvents by imposing an external force ultrasonication or mechanical stirring. Besides the mechanical approaches, chemical approaches such as surface functionalization (Hu et al. 2018; Van den Broeck et al. 2019) and surfactant stabilization (Rassu et al. 2016) are often adopted to disperse inorganic materials uniformly with hydrogel precursor solution. It should be noted that the uniform dispersion of inorganic materials in a solvent does not guarantee a similar dispersion state in the resulting hydrogel composites. Impregnation is such a technique that pure hydrogel synthesized first is immersed into inorganic materials solution to obtain hydrogel composites, or into ion solution followed by being deposited by electrospinning (Im et al. 2010) or precipitation (Li et al. 2019; Pourjavadi et al. 2019) to obtain well-dispersed nanoparticles (NPs) which are embedded in hydrogel networks. This review will mainly focus on the addition of inorganic materials into hydrogels and consequently the property changes in mechanical strength, swelling ratio, and adsorption capability toward aqueous pollutants (Table 1).

Mechanical strength Carbon materials, including graphene, graphene oxide (GO), and carbon nanotubes (CNTs) (Alam et al. 2018), have been the center of intensive research because of their unique structure and technologically useful properties. For example, starch hydrogel presented enhanced mechanical performance, antimicrobial activity, and increased conductivity values by introduction of graphene (Gonzalez et al. 2018). Gelatin–GO hydrogel exhibited a significant increase in mechanical properties by up to 288% in compressive strength, 195% in compressive modulus, 267% in compressive fracture energy, and 160% shear storage modulus with the optimal GO concentration (Piao and Chen 2017). Qin et al. proposed a CS–GO hydrogel composite and it showed 76% increases in the Young's modulus with the addition of 0.5 wt% GO (Qin et al. 2018). Huang et al. found that addition of GO into CS hydrogel could increase compressive strength and work of compression (Huang et al. 2018b). Not only the mechanical property but also the thermal property was improved by the introduction of GO into PAA/amylose hydrogel (Abdollahi et al. 2018).

Clay is another commonly used material for improving the mechanical property of hydrogels. For example, PAM–calcium hydroxide nanospherulites (CNS) hydrogel exhibited excellent mechanical behavior even considering low CNS content. Such gel could sustain high compressive stress at 97% strain and revert to its original size in 1 s after loading was released (Hu et al. 2019a). The same phenomenon could be found in cellulose–MMT (Peng et al. 2016) and PAM–silica NP hydrogels (Zareie et al. 2019). TiO_2 added into SA/PAA (Thakur et al. 2016), poly(N,N-dimethylacrylamide) (PDMAA) (Liao et al. 2014), κ-carrageenan/xanthan/gellan (Balasubramanian et al. 2018), and CS (Liu et al. 2018c; Montaser et al. 2018; Ramos et al. 2016) can strengthen hydrogels' mechanical properties. TiC (Hu et al. 2019b) and tannic acid-modified Fe_3O_4 (Fe_3O_4@TA) (Hu et al. 2018; Liao and Huang 2019a) enhanced both mechanical strength and thermal stability. Of course, the strength of hydrogels is related with the amount of additives. The Young's modulus of PVA/iota–carrageenan increased by the addition of 0.25%

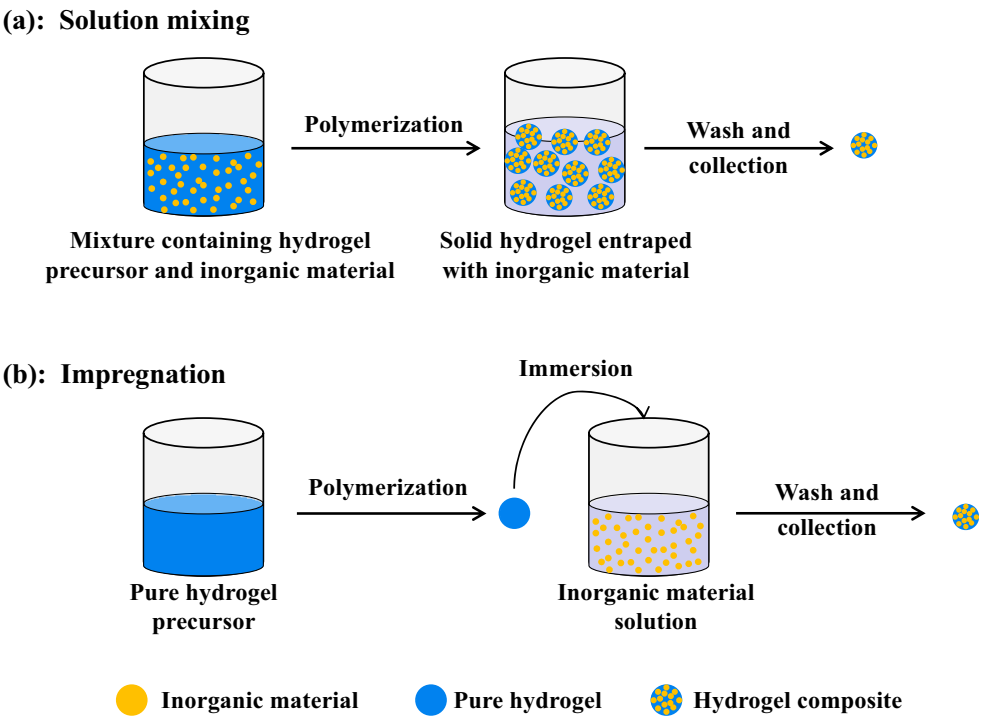

Fig. 2 Two major synthesis routes of inorganic hydrogel composite. **a** Solution mixing. **b** Impregnation

TiO_2, but it decreased with a further increase of TiO_2. Tensile stress and breaking stress behave similarly (Badranova et al. 2016). Although the fraction of additives is critical, it is usually not proportionate to mechanical properties, so the fraction should be adjusted to obtain a balance.

Swelling ratio The swelling behavior of hydrogel is influenced by the presence of inorganic materials and usually decreases with the addition of inorganic materials, which means increased crosslinking degree and mechanical strength. Workers found that the GO embedded into gelatin/polyethylene glycol diacrylate (PEGDA) (Mamaghani et al. 2018) or cellulose/PAA/PAM (Dai et al. 2019) decreased their swelling ratios. The addition of MWCNTs also decreased the swelling ratio of hydrogels (Liu et al. 2019c; Mohammadinezhad et al. 2017). By increasing the dosage of carbon dots (CDs) from 0 to ~ 1%, the swelling ratio of keratin/PVA hydrogel was decreased (Lee et al. 2017). The halloysite nanotubes (HNTs) imbedded into CS/cellulose (Kumar et al. 2019) or SA (Huang et al. 2017) could improve the mechanical property and decrease the swelling ratio. Dargahi et al. prepared κ-carrageenan hydrogel first, and the swollen hydrogel was immersed in silver nitrate solution followed by transferring to sodium chloride solution, and thus, AgCl NPs were introduced, leading to the decreased swelling ratio compared with pure hydrogel (Dargahi et al. 2018). By introduction of Fe_3O_4 NPs into salecan, water uptake was decreased also (Hu et al. 2018).

Generally, the inorganic material plays a reverse role in the swelling ratio that usually decreases with the addition of inorganic material as presented above. However, there are exceptions, for example, the swelling ratio of PVA hydrogel increased by 56.3% with only 1 wt% boron nitride nanofibers added (Li et al. 2018). E-glass fiber (Martin and Youssef 2018), acid-activated MMT (Vieira et al. 2018), ZnO, and PEG-functionalized CNTs (Van den Broeck et al. 2019) increased the swell ratio of hydrogels. Qin et al. found that the average pore diameter and porosity was increased by adding GO into CS, leading to the reduction of swelling ratio (Qin et al. 2018). But the opposite results were obtained by Saravanan et al. who revealed that the addition of GO into CS decreased the porosity and increased the swelling ratio (Saravanan et al. 2018). The addition of TiO_2 into κ-carrageenan, xanthan gum, or gellan gum (Balasubramanian et al. 2018) and PEGylated CS (Liu et al. 2018c) reduced the swelling ratio, whereas it was increased when embedding TiO_2 into collagen/CS (Zazakowny et al. 2016). These different results may be caused by different interactions between water and various hydrogel composites. It is important to note that the swelling characteristics are related to the concentration of additives. Ding et al. prepared PAM–Fe(III) hydrogels by immersing the PAM hydrogel in various concentration of $FeCl_3$ solutions based on coordination complex. The water content of PAM–Fe(III) hydrogels first decreased and then increased as $C_{Fe(III)}$ increased from 0.01 to 0.25 M achieving the minimum value at $C_{Fe(III)} = 0.05$ M (Ding et al. 2019).

Adsorption capability The addition of inorganic materials into hydrogels usually improves the adsorption capability. The amount of Cu(II) adsorbed by PAM/SA–MWCNTs was 1.28

Table 1 Hydrogel composites based on different inorganic materials and methods

Hydrogel composites	Synthesis methods	Surface chemistry	Property enhancement	References
1. C-based composites				
Starch–graphene	Entrapment	/	The hydrogel composite presented enhanced mechanical performance (by the addition of 0.2 wt% of graphene, G' increased from 3660 ± 352 to 5680 ± 362 Pa).	Gonzalez et al. (2018)
Gelatin–GO	Entrapment	Gelatin–GO hydrogel was synthesized using glutaraldehyde-grafted GO as double chemical crosslinkers. The remaining aldehyde groups on the glutaraldehyde-modified GO acted as multiple crosslinker points for further reaction with gelatin chains to yield Schiff base and to create a network.	The hydrogel composite exhibited significant increases in mechanical properties by up to 288% in compressive strength, 195% in compressive modulus, 267% in compressive fracture energy, and 160% shear storage modulus with the optimal GO concentration.	Piao and Chen et al. (2017)
CS–GO	Entrapment	/	• The mechanical strength was improved (The storage (G')/loss (G'') moduli of the hydrogels with different amounts of GO were 1.12 to 1.69 times that of CS. The Young's modulus of 0.5% CS–GO hydrogel is 0.76 times higher than that of CS), and water uptake was reduced slightly. • The gelation time was significantly reduced with the addition of GO (0.5%). • The average pore diameter and porosity was increased by the addition of a small amount of GO (0.5%).	Qin et al. (2018)
CS–GO	Entrapment	As the GO was introduced, the gel composite became relatively dense, which was probably attributed to the intermolecular interactions between the negatively charged GO and the hydrophilic polymer network through physical or chemical bonding.	The hydrogel composite exhibited increased properties in the compressive strength (For the composite with 0.1 wt% GO, the compressive strengths at 60 and 80% strains were 44 and 26% higher than those of the neat gel, respectively).	Huang et al. (2018b)
PAA–GO	Entrapment	The peaks at the 550~650 cm^{-1} by FTIR confirmed the formation of hydrogen bond between GO and PAA.	The hydrogel composite induced the significant improvement in thermal and mechanical properties (By adding 5 wt% GO into PAA, the values of elongation at break decreased from 84 to 22.19%. The elastic modulus of the composite increased from 1.9 to 3.3 GPa. The tensile strength of PAA–GO was 37.1 MPa, whereas the pristine hydrogel was 19.07 MPa).	Abdollahi et al. (2018)
CS–GO	Entrapment	/	The addition of GO decreased the porosity and weight loss and increased the swelling ratio.	Saravanan et al. (2018)
Gelatin methacrylate/PEGDA–GO	Entrapment	/	The swelling ratio was decreased by adding GO.	Mamaghani et al. (2018)
Cellulose/PAA/PAM–GO	Entrapment	The direct esterification reaction between –OH groups of GO and –COOH groups of polymer chains probably	• GO enhanced thermal stability and induced a porous structure of the hydrogel. • The addition of GO decreased swelling ratio and enhanced MB adsorption ability from 75.81 to 133.32 mg/g.	Dai et al. (2019)

Table 1 (continued)

Hydrogel composites	Synthesis methods	Surface chemistry	Property enhancement	References
		existed. GO can also act as a crosslinking agent through strong hydrogen bonding between the –COOH or –OH on GO and $–CONH_2$ on polymer chains.		
CS–GO	Entrapment	/	Introducing GO into CS hydrogel enhanced the mechanical strength (The compressive modulus of the CS–GO was significantly improved with respect to pristine systems by about 200%), and the adsorption of MB was increased from 4.3 ± 1.6 to 168.6 ± 9.6 mg/g with respect to pristine CS.	Salzano de Luna et al. (2019)
SA/PVA–GO	Entrapment	GO could be well integrated with the polymer matrix due to its sheet-like properties, which provided maximal surface area for π–π stacking with polymer hosts. The –COOH and –OH on the edges of GO can also act as linkers for joining polymer.	The MB adsorption was increased by the addition of GO from 1437.48 to nearly 2500 mg/g.	Kong et al. (2019b)
SA/PVA–GO	Entrapment	The presence of GO offered hydrogen bonding interaction between GO and SA/PVA chains. Therefore, GO sheets worked as additional crosslinking points in SA/PVA hydrogels, which was confirmed by FTIR and SEM.	• With increasing GO contents, the SA/PVA composites exhibited smaller pore size; • The addition of GO increased the adsorption of MB from 235 to 247 mg/g due to higher porosity, larger specific area, and a vast number of –OH and –COOH in GO sheets.	Liu et al. (2018a)
Cellulose–GO	Entrapment	Hydrogen bonding was formed between –OH of cellulose and GO.	The addition of GO improved the swelling ratio of hydrogel, and the adsorption capacity of MB was increased from 101 to 138 mg/g.	Geng (2018)
Selenocarrageenan–GO	Entrapment	Hydrogel was formed between GO and selenocarrageenan via the hydrogen bonding and π–π stacking.	The addition of GO improved the adsorption capacity of Hg(II).	Zhuang et al. (2019)
PEG–MWCNTs	Entrapment	The pristine MWCNTs were physically entrapped in the PEG hydrogels and not covalently bound to the hydrogel network.	The hydrogel composite showed significant increase in storage modulus (Rheology showed a significant increase in storage modulus (G') from 1196.7 ± 125.0 Pa for the pure PEG hydrogel to 1915.0 ± 101.7 Pa for the hydrogels with 0.015 wt% pristine CNTs. The compression modulus increased from 4660.0 ± 430.0 to 7320.0 ± 790.0 Pa when adding 0.015 wt% pristine CNTs), and the swelling ratio was decreased slightly by adding pristine CNTs, but increased by PEG-functionalized CNTs.	Van den Broeck et al. (2019)
PAA/poly itaconic acid–MWCNTs	Entrapment	/	• The stability of the hydrogel increased by adding MWCNTs. • The swelling ratio of the hydrogel decreased, and the adsorption behavior toward Pb(II) was improved.	Mohammadinezhad et al. (2017)
Carboxymethyl xylan/PAA–MWCNTs	Entrapment			Liu et al. (2019d)

Table 1 (continued)

Hydrogel composites	Synthesis methods	Surface chemistry	Property enhancement	References
		Hydroxylated MWCNTs interacted with –OH of polymers to form hydrogen bonding.	With increasing of hydroxylated MWCNT concentrations, the network structure of hydrogel became denser, consequently resulting in a lower degree of swelling ratio.	
PAM/SA–MWCNTs	Entrapment	/	The adsorption capacity of Cu(II) by PAM/SA–MWCNTs composite (46 mg/g) was 1.28 times higher than that of PAM/SA (36 mg/g).	Yue et al. (2019b)
XG/PAA–MWCNTs	Entrapment	/	The hydrogel composite exhibited a dramatic increase in hydrophilicity, and the adsorption of MB increased from 79.9 to 133.1 mg/g at 30 °C by adding oxidized MWCNTs.	Makhado et al. (2018)
Keratin/PVA–CDs	Entrapment	Hydrogen bonding between surface functional groups of CDs and available functional groups of keratin/PVA hydrogel was formed and that was confirmed by FTIR.	• As compared to the pure hydrogel, the hydrogels with CDs possess more fibrous morphology. • Swelling ratio was decreased by increasing the dosage of CDs from 0 to 1%.	Lee et al. (2017)
2. Si-based composites				
SA/AM–SiO_2	Entrapment	The vinylated SiO_2 microspheres were covalently crosslinked with hydrogel.	The removal efficiency of MB increased from 62 to 139.31 mg/g by adding vinylated SiO_2.	Panão et al. (2019)
SA/PAM–E glass fiber	Entrapment	/	• The storage moduli gained a 75% increase in response to 3 wt% E-glass fiber for SA/PAM. • Swelling ratio was increased by adding E-glass fiber.	Martin and Youssef (2018)
CS–fumed nanosilica	Entrapment	/	Adding APTS-modified fumed nanosilica into CS enhanced the adsorption capacities of Co(II), Cu(II), Pb(II), and Zn(II).	Pourjavadi et al. (2015)
PAM–fumed silica	Entrapment	/	The addition of fumed silica NPs increased the crosslink density of hydrogel and mechanical strength (The strain modules of hydrogel which were filled by silica nanoparticles of 9 wt% are reduced in strain of 100 to about 3000% without breaking. The elastic modulus was increased in the presence of silica nanoparticles more than 5000% in strain of 1%), but reduced the swelling ratio.	Zareie et al. (2019)
3. Clay-based composites				
PAM–CNS	Entrapment	Carboxyl (–COOH) hydrolyzed by side chain ($CONH_2$) of PAM reacted with CNS to form $–COO^{-}Ca^{2+}$, which was proved by time of flight secondary ion mass spectrometry.	The hydrogel composite exhibited excellent mechanical behavior even considering low CNS content and can sustain high compressive stress at 97% strain.	Hu et al. (2019a)
PVA/SA/CS–MMT	Entrapment	The chains of PVA, SA, and CS entangled together and formed the net by hydrogen bonding and electrostatic interaction, then the MMT as the enhancer could combine along the CS chain and formed the huge plane.	The MB removal rate was 90% by hydrogel beads with MMT amount of 29.70%, while it was 68.16 and 42.46% with MMT amounts of 17.44 and 9.55%, which indicated MMT could enhance the removal rate of MB on hydrogel beads.	Wang et al. (2018d)
Cellulose–MMT	Entrapment			Wang et al. (2019c)

Table 1 (continued)

Hydrogel composites	Synthesis methods	Surface chemistry	Property enhancement	References
		FTIR revealed a strong hydrogen bonding interaction between cellulose and MMT.	The adsorption capacities of MB at pH 7 were 177, 205, and 254 mg/g for the concentration of MMT 5, 10, and 20 wt%, respectively.	
CS–MMT	Entrapment	Hydrogen bond and electrostatic interaction generated the hydrogels. There were abundant Al–OH groups on the edge of MMT, while CS possessed lots of –NH groups on the chain.	Pb(II) adsorption performance was improved by increasing the ratio of MMT.	Wang et al. (2019d)
CS–MMT	Entrapment	/	Swelling degree was improved by adding acid-activated MMT.	Vieira et al. (2018)
Carboxymethyl cellulose/CS-HNTs/GO	Entrapment	The suggested chemistry of the used materials was ionic crosslinking, weak electrostatic interactions, and hydrogen bonding.	• The incorporation of HNTs improved the compressive strength (from 18.26 to 20.51 kPa) and stiffness values (from 730.1 ± 42.3 to 1237.0 ± 48.9 N/m) of hydrogel composites with increasing of amount of HNTs (from 1 to 10 wt%). • The swelling ratio of the hydrogels was decreased after the incorporation of HNTs.	Kumar et al. (2019)
SA–HNTs	Entrapment	The hydrogen bond was formed between SA and HNTs which was confirmed by FTIR.	• The compressive mechanical property (The hydrogel composite with 80% HNTs loading exhibited the compressive stress of 2.99 MPa at 80% strain, while the stress at 80% strain of pure SA hydrogel was 0.8 MPa) and storage modulus (The G' of the SA hydrogel at 0.1% strain was 16,413.0 Pa, while hydrogel composite was 5.3-folds of that of pure SA hydrogel) of hydrogel composite increased by the addition of HNTs. • The swelling ratio was decreased.	Huang et al. (2017)
PAA–HNTs	Entrapment	/	Hydrogel composite showed better adsorption of RhB than the bare PAA hydrogels, but it would decrease if the loading of HNTs was above 1 mg per 30 mg PAA.	Bethi et al. (2018)
PAM–layered double hydroxide (LDH)	Entrapment	The interactions between PAM and LDH nanosheets may include coordination interaction between $C(O)NH_2$ and LDH edge metal ions (Co^{2+} and Al^{3+}) and hydrogen bonding interaction between $–C(O)NH_2$ in the PAM chain and –OH on LDH.	The equilibrium adsorption amount of MO was 21.65 mg/g by hydrogel composite.	Yang et al. (2019b)
4. Metal-based composites				
CS–Ag^+–NH_3	Entrapment	The formation of CS–Ag^+–NH_3 hydrogel was a self-assembly process and Ag^+ functioned as a physical crosslinker to form noncovalent coordinate bonds with CS. Ammonia gas worked	The tensile strength of the CS–Ag^+–NH_3 hydrogels increased with the increase of Ag^+ concentrations and the ultimate stress was 0.17 MPa.	Li et al. (2017)

Table 1 (continued)

Hydrogel composites	Synthesis methods	Surface chemistry	Property enhancement	References
		as a pH regulator to neutralize the acidic CS solutions to initiate the gelation.		
k-Carrageenan–AgCl	Precipitation	The silver ions were localized throughout the hydrogel networks due to a strong interaction with the sulfate, hydroxyl, and carboxylate groups in the hydrogel network.	The swelling ratio was reduced, and the adsorption capacity of crystal violet was increased from 77.22 to 96.84 mg/g due to the presence of AgCl.	Dargahi et al. (2018)
Salecan/poly(hydroxypropyl methacrylate)–TiC	Entrapment	The interactions of polymer chains with TiC induced molecular stiffening and the consequent rearrangement of polymer structure, which led to the change in the structure of the composite hydrogels.	The addition of TiC enhanced the mechanical strength (The value of G' was increased from 450.4 to 1367.2 Pa. The fracture stress of hydrogel composite was up to 69,700 Pa, much larger than that of the bare hydrogel (21,400 Pa)) and thermal stability.	Hu et al. (2019b)
Salecan–Fe_3O_4@TA	Entrapment	Fe_3O_4@TA nanoparticles were dispersed in the copolymer network and hydrogen bonds could be established between the functional groups of copolymer chains and Fe_3O_4@TA, which was confirmed by the FTIR and XRD analysis.	• Salecan and salecan–Fe_3O_4@TA exhibited compressive modulus of 2030 and 4840 Pa, respectively, and the storage moduli increased from 680 ± 16.2 to 1496 ± 29.1 Pa due to the presence of Fe_3O_4@TA. • The swelling ratio was decreased.	Hu et al. (2018)
Chitin/PVA–Fe_3O_4	Precipitation	Strong interactions between the –OH groups of polymer and Fe_3O_4 occurred.	The hydrogel composite displayed superparamagnetic behavior and improved strength (The storage modulus (G') of the hydrogel composite was clearly higher than pure hydrogel. The fracture strain and stress for pure hydrogel were 58% and 0.09 MPa, but increased to 66% and 0.19 MPa after being loaded with Fe_3O_4).	Liao and Huang (2019a)
Chitin–Fe_3O_4	Precipitation	/	The Cu(II) adsorption capacity was enhanced from 10.65 to 35.39 mg/g in the presence of Fe_3O_4 due to the high surface area and affinity toward Cu^{2+} of Fe_3O_4.	Liao and Huang (2019b)
PVA/CS–Fe_3O_4	Entrapment	/	The addition of Fe_3O_4 containing polyamide 6 into the hydrogels resulted in an increase of the Cu(II) adsorption efficiency from 38.7 to 43.4 mg/g.	Wu et al. (2019a)
Starch–ZnO	Precipitation	Because of the porous construction of starch hydrogels and the presence of $–CH_2O^-$ and $–CO_2^-$, the oxidized starch hydrogels bound to the zinc ions through electrostatic connection. Zinc ions are oxidized to ZnO NPs with NaOH.	Swelling ratio was increased by adding ZnO.	Namazi et al. (2019)
CS–ZnO	Precipitation	Zinc ions were bound onto the negatively charged carboxylic group (COO^-) of the CS hydrogel via electrostatic force.	The carboxymethyl CS–ZnO hydrogel composite showed rather higher swelling behavior in comparison with neat hydrogel.	Wahid et al. (2016)
SA/PAA–TiO_2	Entrapment	/		Thakur et al. (2016)

Table 1 (continued)

Hydrogel composites	Synthesis methods	Surface chemistry	Property enhancement	References
			The storage modulus was increased from 5120 to 9810 MPa by adding TiO_2.	
k-Carrageenan/XG/gellan gum–TiO_2	Entrapment	It confirmed the covalent interactions formed between TiO_2 and κ-carrageenan /XG/gellan gum materials (The adsorption band of the –OH or –CH bending at 1460 cm^{-1} and C–O–H at 1157 cm^{-1} for the κ-carrageenan /XG/gellan gum shifted to lower wave number of 1147 and 1152 cm^{-1}, respectively, confirming the possible interaction between TiO_2 and κ-carrageenan/XG/gellan gum).	The tensile strength and tensile modulus of the hydrogel composite increased 39 and 122%, respectively, with the addition of TiO_2 (7 wt%).	Balasubramanian et al. (2018)
CS–TiO_2	Entrapment	Ti is a lanthanide metal having a vacant orbital; thus, hydrogen atom from –OH group of the glycoside ring of CS can make a coordination bond with Ti and form a complex.	Improvement of thermostability and mechanical property (tensile strength increased from 1.36 to 4.50 kg) in the presence of TiO_2 was observed.	Montaser et al. (2018)
CS–TiO_2	Entrapment	No new bands could be observed on the CS–TiO_2 spectrum, which indicated that no new chemical groups were formed during the hybrid synthesis.	The storage modulus increased with the raise of TiO_2 content.	Ramos et al. (2016)
CS–TiO_2	Precipitation	The characteristic peaks at 1650 and 1440 cm^{-1}, which is corresponding to the symmetric and asymmetric COO^- groups, respectively, slightly shifted to a higher wavenumbers, due to the interaction of TiO_2 NPs with functional groups of CS.	• The homogeneous incorporation of TiO_2 NPs into the PEGylated CS hydrogel networks led to an increase in Young's modulus from 430 kPa to a maximum of 1500 kPa related to the concentration of TiO_2 NPs. • Decreased swelling ratio was observed by adding TiO_2.	Liu et al. (2018c)
PVA/iota–carrageenan–TiO_2	Entrapment	/	The Young's modulus was increased from 1655.85 to 2055.3 MPa by the addition of 0.25% TiO_2, but it decreased with a further increase of TiO_2.	Badranova et al. (2016)

Note: "/" means surface chemistry was not mentioned in the reference

times higher than that of PAM/SA owing to its multiwalled hollow nanostructure (Yue et al. 2019b). Adding MWCNTs into hydrogels also showed better adsorption behavior toward Pb(II) (Mohammadinezhad et al. 2017) and MB (Makhado et al. 2018) than pure hydrogels. The dyes of MB (Dai et al. 2019; Geng 2018; Kong et al. 2019b; Liu et al. 2018a; Salzano de Luna et al. 2019; Zhuang et al. 2019) and Nile Red (Sun et al. 2018) adsorbed by hydrogels were largely increased by adding GO. Metal ions, such as Cu(II) (Geng 2018) and Hg(II) (Zhuang et al. 2019) adsorbed by cellulose or selenocarrageenan hydrogels, were also improved due to the presence of GO.

Besides carbon-based materials, SiO_2 NPs can also enhance hydrogels' adsorption capacity for removal of MB (Panão et al. 2019) and metal ions such as Co(II), Cu(II), Pb(II), and Zn(II) (Pourjavadi et al. 2015). The addition of MMT into PVA/SA/CS (Wang et al. 2018d) or cellulose (Wang et al. 2019c) could enhance the adsorption of MB. Also, the adsorption of Pb(II) was enhanced by adding MMT into CS hydrogel (Wang et al. 2019d). The addition of HNTs into the PAA hydrogel showed better adsorption of rhodamine B (RhB) than the bare PAA hydrogel (Bethi et al. 2018). Metal compound NPs can also be used as hydrogel fillers. The addition of AgCl NPs into κ-carrageenan hydrogel showed better adsorption toward crystal violet (Dargahi et al. 2018). By imbedding Fe_3O_4 NPs into chitin (Liao and Huang 2019b) or PVA/CS (Wu et al. 2019a), the Cu(II) adsorption capacity was enhanced.

These inorganic fillers are responsible for the significant improvement of mechanical and functional properties. It is worth noting that some inorganic materials not only provide a strong support to hydrogels and change the swelling ratio and adsorption capability, but also help to form hydrogel networks, such as GO, which acted as multifunctional crosslinking sheets and reduced the gelation time by nearly 20% only with a small amount of GO (0.5% weight ratio of CS into CS) (Qin et al. 2018). The same phenomenon was found in MMT which can also reduce the cellulose gelation time (Peng et al. 2016). Layered double hydroxide (Yang et al. 2019b) and Al_2O_3 NPs (Xu et al. 2018) could also be used as crosslinking agents. This phenomenon was more evident for TiO_2 which can be used as light initiator to totally replace conventional chemical crosslinking agents (Glass et al. 2018; Kangwansupamonkon et al. 2018). These studies confirm that some inorganic materials can act as an effective physical crosslinker for hydrogel synthesis, reduce the gel time, and improve the properties of hydrogels in the meanwhile.

Application of hydrogels

Hydrogels used as adsorbents

Adsorption capacity The reported adsorption capacities for ECs are summarized in Table 2. The adsorption process strongly depends on the type of ECs as well as the hydrogel adsorbents. The maximum adsorption capacity of various hydrogels for BPA in water at the best conditions was between several and hundred milligrams per gram of adsorbents after tens of minutes of reaction. But much time was necessary if the size of hydrogels was too big to mass transfer quickly (Luo et al. 2019). The maximum adsorption capacities of ciprofloxacin (CIP) were 100, 154.89, and 200 mg/g for SA–GO bead, CS–biochar bead and κ-carrageenan/SA bead (Zhao et al. 2018b; Afzal et al. 2019; Yu et al. 2019), respectively. The PNIPAAM/CS–Fe_3O_4 hydrogel showed maximum adsorption capacities of 164.3 mg/g for BPA, while that for sulfamethoxazole (SMZ) was 15.7 mg/g (Zhou et al. 2019). However, SMZ adsorbed by poly(2-hydroxyethyl methacrylate)/poly(N-methyl maleic acid)–CuS (PHEA/PNMMA–CuS) hydrogel was 3.86 mg/g (Yang et al. 2017). Diclofenac sodium (DS) adsorbed by CS–Fe_3O_4 and SA/cellulose/PVA were 469.48 mg/g (Liang et al. 2019a) and 418.41 mg/g (Fan et al. 2019), respectively. It is worth mentioning that the environmental parameters such as pH, initial pollutant concentration, and adsorbent dose are critical factors which show significant effects on ECs' adsorption capacity.

Removal mechanism As presented in Table 2, the adsorption data of ECs on hydrogels can be well interpreted by the Freundlich model or Langmuir model, with the kinetic model being pseudo-second-order in most cases. Hydrogel-based adsorbents have strong affinity for ECs, mainly due to the diverse interactions of these adsorbates with the adsorbents, including hydrophobic interaction, electrostatic interaction, hydrogen bonding, and π–π interaction, which varies according to the adsorbent, chemical nature of the adsorbate, pH, the ionic strength of the solution, and so on.

Hydrophobic interaction Hydrophobic interaction is the main mechanism responsible for the hydrophobic organic compounds. The maximum amount of CIP adsorbed by SA–GO hydrogel occurred at neutral pH of 7.0, when CIP was in zwitterionic form. At this pH, SA–GO can provide more hydrophobic sites, which in turn increased the hydrophobic interaction between SA–GO and CIP molecules (Zhao et al. 2018b). It also played a crucial role in CIP adsorption on the surface of humic acid-modified CS–biochar (Afzal et al. 2019). Due to the hydrophobicity of BPA, hydrophobic interaction between BPA and the hydrophobic group isopropyl of PNIPAAM/CS–Fe_3O_4 might occur. With an increase in pH, BPA molecules were dissociated, which led to the destruction of hydrophobic interaction and, thus, a decrease in BPA adsorption (Zhou et al. 2019).

Electrostatic interaction Electrostatic interaction is another mechanism for hydrogel materials to adsorb ECs. When the solution pH is different from the isoelectric point (pHpzc) of

Table 2 Adsorption behavior of ECs from aqueous solution by hydrogel adsorbents

Hydrogel	ECs	Initial concentration of ECs (mg/L)		q_e (mg/g)	t_e (min or h)	Kinetic model	Isotherm model	Adsorptive mechanism	References
Cellulose	BPA	99.54		14.6	90 min	Pseudo-second-order	Freundlich	/	de Souza and Petri (2018)
PHEA/PHAM–CdS	BPA	50		11.26	10 min	Pseudo-second-order	Langmuir	/	Zhu et al. (2018)
PNIPAAM/CS–Fe_3O_4	BPA	100		164.3	/	Pseudo-second-order	Freundlich	Hydrophobic interactions, hydrogen bonds	Zhou et al. (2019)
Xanthan/NIPA	BPA	800		458	/	Pseudo-second-order	Freundlich	/	Chen et al. (2019)
PEGDA/PEGMA	BPA	1000		174.77	15 min	Pseudo-second-order	Freundlich	/	Du and Piao (2018)
Cellulose	BPA	200		30.77	/	Pseudo-second-order	Langmuir	/	Lin et al. (2019b)
SA/CS-MOF	BPA	120		136.91	17 h	Pseudo-second-order	Freundlich	π–π stacking, hydrogen bonding	Luo et al. (2019)
k-Carrageenan/SA	CIP	400		229	48 h	Pseudo-second-order	Langmuir-Freundlich dual site	/	Yu et al. (2019)
SA–GO	CIP	50		100	72 h	Pseudo-second-order	Freundlich	Hydrophobic interaction, ion exchange	Zhao et al. (2018b)
CS–biochar	CIP	250		154.89	12 h	Pseudo-second-order	Langmuir	Hydrogen bonding, π–π stacking, hydrophobic interactions	Afzal et al. (2019)
CS–Fe_3O_4	DS	800		469.48	60 min	Pseudo-second-order	Langmuir	Electrostatic interactions, hydrogen bonding	Liang et al. (2019a)
SA/cellulose/PVA	DS	840		418.41	50 min	Pseudo-second-order	Langmuir	Electrostatic interactions, hydrogen bonding	Fan et al. (2019)
PNIPAAM/CS–Fe_3O_4	SMZ	10		15.7	/	Pseudo-second-order	Freundlich	Electrostatic attraction	Zhou et al. (2019)
PHEA/PNMMA–CuS	SMZ	50		3.86	4 h	Pseudo-second-order	/	/	Yang et al. (2017)

q_e, adsorption capacity; t_e, equilibrium time

hydrogel adsorbents, the surface of hydrogel adsorbents will carry either a positive or negative charge. At the same time, ionizable ECs can also be protonated or deprotonated and become charged at different pH values, and the resulting electrostatic interactions between them may influence the adsorption property of ECs. The amount of DS adsorbed by humic acid-modified CS–Fe_3O_4 hydrogel decreased with increasing pH, owing to repulsive electrostatic interactions between the negative surface charge of hydrogel and the negatively charged anionic form of DS ($–COO^{-1}$ and $–O^{-1}$). When pH < pHzpc, the CS–Fe_3O_4 surface had a positive charge and can adsorb negatively charged DS. However, when pH > pHzpc, the CS–Fe_3O_4 surface had a negative charge, which cannot attract DS with a negative charge on the surface (Liang et al. 2019a). Fan et al. found that the SA/CNC/PVA hydrogel surface charge was positive when pH < 5.3, and when pH > 5.3, the surface charge was negative. The –COOH in DS was ionized when pH > 4, mainly in the form of anions. Therefore, when the pH was between 4.2 and 5.3, the positively charged surface of SA/CNC/PVA had electrostatic interactions with anionic DS. At pH > 5.3, the adsorption capacity decreased sharply, mainly because the repulsion force between SA/CNC/PVA and DS in anionic form increased (Fan et al. 2019). For SMZ, the adsorption capacity by CS hydrogel reached maximum at an equilibrium pH of around 6 and decreased on either side of this range. The amino groups of CS were protonated under acidic condition, which caused the adsorbent to be positively charged, and thus, anionic SMZ^- as the predominant species under pH 6 formed the electrostatic attraction with positively charged adsorbent. With the pH increasing, the positive charge of the hydrogels decreased, leading to the reduction of electrostatic attraction and, thus, a decrease in the adsorption capacity (Zhou et al. 2019).

Hydrogen bonding Hydrogen bonding is a vital aspect for the successful adsorptive removal of ECs by hydrogel adsorbents. pH is an important factor affecting adsorption mechanism. When the pH exceeded the pHpzc of SA/CNC/PVA, acid–base interactions decreased, and negatively charged SA/CNC/PVA and DS mainly reacted via hydrogen bonding interactions (Fan et al. 2019). During the adsorption of SMZ by PNIPAAM/CS–Fe_3O_4, neutral molecules were the predominant form of SMZ at pH < 6; thus, electrostatic attraction was less likely to occur. However, a little adsorption capacity still existed, indicating that there might be hydrogen bonds formed by the sulfonamide groups of SMZ as well as the –NH and –OH of CS (Zhou et al. 2019). The BPA can be adsorbed by SA/CS–MOF due to the formation of hydrogen bonds between oxygen atoms in the −COO of SA/CS–MOF and −OH of BPA, which was confirmed by full-scale XPS pattern, because the proportion of −COO in SA/CS–MOF was detected lower after adsorption (Luo et al. 2019).

During the adsorption of CIP by CS–biochar hydrogel, some functional groups in CIP, such as −NH and −OH, acted as hydrogen bond donors and some acted as hydrogen bond acceptors, such as the benzene ring. Another possible hydrogen bond can occur between the −OH present on the surface of CS–biochar and polar CIP functional groups, such as F, N, and O, which acted as hydrogen bond acceptor (Afzal et al. 2019).

π–π interaction Considering the presence of benzene rings in both BPA molecules and the SA/CS–MOF, π–π interactions may occur during the process of BPA adsorption (Luo et al. 2019). A similar mechanism was reported for CS/biochar for adsorption of CIP which also contains a benzene ring (Afzal et al. 2019).

Desorption studies Desorption is important in the field of actual application, and the choice of elution solvent is very significant. Under a given desorption condition, the interaction of ECs with the binding sites on the polymer surface could be disrupted, and subsequently, EC molecule was released from the polymer into the desorption medium. In order to strengthen the mass transfer, ultrasonic or shaking is usually needed during the desorption process.

As one of the most detected ECs in aquatic environment, BPA did not dissolve completely in pure water due to its low water solubility. So, organic solvents are often used as regeneration liquid. Methanol is the most common option. The desorption of cellulose hydrogel bead was investigated by Lin and coworkers. After adsorption, the cellulose hydrogel bead saturated with BPA was added into methanol solution in a thermostatic water bath shaker at 25 °C for 2 h, and the adsorption capacity was 68.11% of the initial after four adsorption/desorption cycles (Lin et al. 2019b). When BPA was adsorbed by PNIPAAM/CS–Fe_3O_4, the adsorption capacity gradually decreased to 94% of the initial in five cycles of adsorption/desorption when methanol was used as the eluent (Zhou et al. 2019). The regeneration of SA/CS–MOF was studied by eluting using methanol, and the adsorption efficiency of BPA on SA/CS–MOF decreased by about 2.4% after the first adsorption/desorption cycle and then remained almost unchanged until the end of the fifth cycle, indicating the high stability and excellent reusability of the SA/CS–MOF (Luo et al. 2019). It is worth noting that different eluents own different elution efficiencies. The authors revealed that the highest desorption efficiency (100%) was obtained by using methanol/dimethylsulfoxide as eluting solution (v:v = 9:1), and the efficiencies were 97 and 98% for ethanol and methanol, respectively (Du and Piao 2018). Adding water to pure organic solvents can reduce regeneration cost without affecting the desorption effect, for example, the cellulose hydrogel kept 90% of the original capacity of BPA after five adsorption/desorption cycles by immersing the BPA-loaded hydrogel in the mixed solvent of ethanol:water (v:v = 3:1) (de Souza and Petri 2018). Zhou et al. have studied the desorption experiment to remove the adsorbed SMZ from PNIPAAM/CS–Fe_3O_4 hydrogel and the spent adsorbent was treated with methanol. The adsorption capacity decreased to 55% of the initial capacity after five cycles of adsorption/desorption (Zhou et al. 2019).

Unlike BPA and SMZ, which often use organic solvent as regeneration liquid due to its low solubility in water, certain ECs can be solved in inorganic solvent perfectly such as acid/alkaline solution or distilled water. To desorb CIP, used humic acid CS–biochar was shaken with 1.0 M NaOH for 30 min in the steam bath vibrator at 250 rpm and then separated for repeated use. The adsorption capacity remained 39.53% as the original capacity after four regeneration cycles (Afzal et al. 2019). For the desorption experiment of DS, saturated CS–Fe3O4 was treated with 0.1 M NaOH for 5 min by ultrasonication and stirring. Then the adsorption capacity was reduced to 45.77% of the original capacity after four cycles (Liang et al. 2019a). In another study, DS-adsorbed SA/cellulose/PVA was subjected to desorption with 0.1 M HCl. After five adsorption/desorption cycles, SA/cellulose/PVA hydrogel showed only a slight loss (11.44%) in adsorption capacity (Fan et al. 2019).

Overall, it was concluded that after several adsorption/desorption cycles, the adsorption capacity of adsorbent declined gradually. Reduction in the surface area and number of functional groups on the adsorbent may result in a decrease in adsorption capacity of hydrogel adsorbent. Besides, the degree of capacity loss is also dependent on the substrate and the eluent.

Hydrogel templates for the synthesis of nanomaterials

During the adsorption process, the pollutants continuously accumulate onto hydrogels until they are fully saturated. These exhausted materials can be either burnt or disposed of in landfills, but this entails environmental concerns. An alternate option which is rather environmentally safe and economically attractive is the reuse of exhausted hydrogels. Recent trends have demonstrated that hydrogels can be used as nanoreactor for in situ synthesis of NPs as the following steps: adsorbents for metal removal, templates for metal NP synthesis, and reactors for pollutant removal. The adsorbed metal ions can be transformed to metal elemental NPs usually by the reduction process, including chemical synthesis (Ilgin et al. 2019; Pourbeyram and Mohammadi 2014; Tang et al. 2018), electrochemical synthesis (Nešović et al. 2018), and photo crosslinking (Ai and Jiang 2013). The oxidation process is (Natkański et al. 2016; Ojeda et al. 2017) often used for metal oxidant NP synthesis. Such findings are encouraging because if hydrogels are highly reusable, it makes the overall process more economical and sustainable.

Ilgin et al. prepared the PAM/N-methacrylamidothiomorpholine hydrogel for selectively adsorbing Au(III) and then they were reduced to Au NPs by $NaBH_4$ reducing agent for degrading 4-NP (Ilgin et al. 2019). The same method was also suitable for reducing Ni, Co (Sahiner et al. 2012), and Pd ions (Yao et al. 2018) to their corresponding NPs. Cu NPs could also be synthesized by reducing adsorbed Cu(II) with $NaBH_4$ (Godiya et al. 2018, 2019; Su et al. 2018) or hydrazine (Pourbeyram and Mohammadi 2014). Besides $NaBH_4$, the metal ions could be reduced by special functional groups which existed in hydrogels themselves. For example, $AgNO_3$ solution was mixed with PVA/CS–graphene or PVA/lignin hydrogel presolution and Ag NPs were synthesized based on the antioxidant properties of CS (Nešović et al. 2018) or lignin (Li et al. 2019). The cellulose with hydroxyl groups could also reduce the Ag ions into Ag NPs (Han et al. 2016) or Ag@AgCl NPs (Tang et al. 2018). The NPs can also be obtained without reducing agents. As examples, Ai et al. dropped SA into Ag solution and then the hydrogel was irradiated with a lamp for 90 s to prepare Ag NPs and used for reduction of 4-NP (Ai and Jiang 2013). CdS was obtained by mixing PAA/PAM hydrogel solution with $CdCl_2$ and $Na_2S_2O_3$, and then irradiated by ^{60}Co gamma rays at room temperature (Yang et al. 2018a). The synthesized PAA–GO hydrogel served as an efficient adsorbent for Cd(II) and as a suitable matrix for the CdS quantum dot formation by in situ precipitated and further used for photocatalyzing MB (Kong et al. 2019a). As for metal oxidant NPs, such as Fe_2O_3 (Natkański et al. 2016) or TiO_2 (Ojeda et al. 2017), the oxidation process is the proper method.

To sum up (Table 3), the hydrogel used as matrix to synthesize metal NPs is just suitable for metal pollutants

Table 3 Hydrogel templates for the synthesis of nanomaterials

Hydrogel templates	Nanomaterials	Synthesis method of nanomaterials	References
PAM	Au	The selectively adsorbed gold (III) ions were reduced by $NaBH_4$ and used for degradation of 4-NP.	Ilgin et al. (2019)
SA/polyethylenimine	Cu	The Cu(II) ions adsorbed by the hydrogel were reduced to Cu NPs by $NaBH_4$, and Cu NPs were used to catalyze 4-NP.	Godiya et al. (2019)
CMC/PAM	Cu	The adsorbed Cu(II) ions were reduced by $NaBH_4$ and the obtained Cu NPs were used for degradation of 4-NP.	Godiya et al. (2018)
PAA	Cu	The hydrogel loaded with Cu(II) ions were reduced to Cu NPs by $NaBH_4$, and Cu NPs were used to catalyze 4-NP and MB.	Su et al. (2018)
PAA	Cu	Cu(II) ions were allowed to diffuse into the water-swollen hydrogel and then reduced to Cu NPs inside the hydrogel networks with hydrazine.	Pourbeyram and Mohammadi (2014)
Poly(sulfopropylmethacrylate)	Ni, Co, and Cu	The hydrogel loading with Ni(II), Co(II), or Cu(II) was reduced by $NaBH_4$ to prepare NPs for reduction of 4-NP and 2-NP.	Sahiner et al. (2012)
Ppy	Pd	The hydrogel served as a support to load Pd nanoclusters and reduced them to Pd NPs by $NaBH_4$.	Yao et al. (2018)
PVA/CS–graphene	Ag	$AgNO_3$ solution was added to the hydrogel presolution and reduced to Ag NPs by electrochemical synthesis in which the CS itself acted as a reducing agent.	Nešović et al. (2018)
PVA/lignin amine	Ag	$AgNO_3$ solution was added to the hydrogel presolution to obtain Ag NPs directly using the antioxidant property of lignin.	Li et al. (2019)
Cellulose	Ag	$AgNO_3$ solution was added to the hydrogel presolution to obtain a hydrogel containing Ag NPs using cellulose as reducing agents for catalyzing 4-NP and MB.	Han et al. (2016)
Cellulose	Ag@AgCl	The adsorbed Ag ion was reduced by hydroxyl groups in cellulose, which facilitate the reduction of surface Ag ions into Ag NPs for photodegradation of MO under visible light irradiation.	Tang et al. (2018)
SA	Ag	SA was dropped into Ag ion solution and then the hydrogel was irradiated with a lamp to prepare Ag NPs for reduction of 4-NP.	Ai and Jiang (2013)
PAA/PAM	CdS	Hydrogel solution mixed with $CdCl_2$ and $Na_2S_2O_3$ was irradiated by ^{60}Co gamma rays to obtain CdS NPs.	Yang et al. (2018a)
PAA–GO–CdS	CdS	The PAA–GO was used to adsorb Cd(II), and then the PAA–GO–Cd(II) was in situ precipitated by Na_2S solution to obtain PAA–GO–CdS composite for photocatalyst of MB.	Kong et al. (2019a)
PAA–MMT	Fe_2O_3	Fe(III) adsorbed by hydrogel was calcined at 600 °C to prepare Fe_2O_3 NPs.	Natkański et al. (2016)
PAA	TiO_2	The titanium (IV) chloride was mixed with AA to obtain PAA hydrogel first, and then the hydrogel loaded with Ti(IV) was calcined at 450 °C to prepare TiO_2 NPs.	Ojeda et al. (2017)

because the adsorbed metal ions could be converted to metal NPs which can be further used as catalyst for pollutant remediation. But as for organic compounds, hydrogels can hardly be recycled in the same way. So, it is necessary to combine the hydrogel and the catalyst, such as chemical catalyst and enzyme, to mineralize

Table 4 Hydrogel matrixes as chemical catalysts carriers

Hydrogel composites	Immobilization methods	Properties	References
1. Photocatalytic hydrogels			
PAA–TiO_2	Entrapment	The reactive blue 4 was adsorbed first and then photodegraded by hydrogel composite.	Yu et al. (2018b)
PAA/PAM/cellulose–TiO_2	Entrapment	• The addition of TiO_2 decreased the swelling ratio and improved the mechanical property of the hydrogel. • RhB was first adsorbed and then photodegraded by the hydrogel composite.	Wang et al. (2018c)
CS/PNIPAAM–TiO_2	Entrapment	The acid fuchsin can be adsorbed by hydrogel composite, and the removal efficiency was enhanced by photocatalytic reaction.	Zhou et al. (2017)
SA/CMC–TiO_2	Entrapment	Congo red was first adsorbed and then photodegraded by hydrogel composite.	Thomas et al. (2016)
PVA/PAA–TiO_2–GO	Entrapment	The dyes (MB and Coomassie brilliant blue R-250) adsorbed by PVA/PAA–TiO_2–GO hydrogel composite increased as the content of GO increased, and the adsorbed dyes could be further photodegraded.	Moon et al. (2013)
PVA–TiO_2	Electrospinning	The dyes (procion blue and acridine orange) were adsorbed to the photocatalyst and then photodegraded.	Im et al. (2010)
CS–TiO_2	Immersion	• Shear modulus was improved and swelling ratio was decreased a little in the presence of TiO_2. • The adsorption capacity of dyes (C.I. Acid Red 18, C.I. Acid Blue 113, C.I. Reactive Black 5, and C.I. Direct Blue 78) was improved due to the TiO_2, and the adsorbed dyes were degraded.	Lučić et al. (2014)
PHEA/APTM–BiOI	Precipitation	The binary mixture of peroxymonosulfate and PHEA/APTM–BiOI removed more than 80% of MP in the absence of visible light.	Hu et al. (2019c)
PHEA/PHAM–CdS	Precipitation	The swelling ratio and adsorption of BPA were higher than pure PHEA/PHAM due to the presence of CdS and showed synergy between adsorption and photocatalytic degradation.	Zhu et al. (2018)
PHEA/PNMMA–CuS	Precipitation	The adsorption of SMZ by PHEA/PNMMA–CuS was higher than pure PHEA/PNMMA and showed synergy between adsorption and photocatalytic degradation.	Yang et al. (2017)
PAM–bentonite–g-C_3N_4	Entrapment	The enhanced removal of TOC is attributed to the synergistic effect of adsorption and photocatalytic degradation.	Hao et al. (2018)
rGH–Ag_3PO_4	Precipitation	The BPA was 100% removed in 12 min by the synergy of adsorption and photocatalysis under visible light irradiation.	Mu et al. (2017)
CS/gelatin–zirconium (IV)	Entrapment	Adsorption and photodegradation of MB by the hydrogel composite was enhanced compared with pure CS/gelatin or pure zirconium (IV) and showed synergy between adsorption and photocatalytic degradation.	Kaur and Jindal (2019)
CS–graphite–La(III)	Entrapment	The highest photodegradation was due to the stronger adsorption of MB on the surface of highly porous hydrogel.	Sirajudheen and Meenakshi (2019)
2. Fenton hydrogels			
CS/SA–Fe(II)	Entrapment	The results demonstrated a much higher removal efficiency of BPA (99.5%) than the conventional Fe(II) system (69.2%) with a negligible amount of Fe ions released into the solution.	Kang et al. (2018)
SA–Fe(II)	Entrapment	The hydrogel catalyst presents good stability and can be used for at least five times without obvious decrease in activity during the Fenton process for removing indole.	Ben Hammouda et al. (2016)
CS/Cu(II)–Fe(III)	Precipitation	The hydrogel composite was used for oxidation of C.I. Reactive Black 5.	Rashid et al. (2015)
rGO/Ppy–Fe_2O_3	Precipitation	The hydrogel composite was used for degradation of MB and showed superior reusability in recycling experiments.	Zhang et al. (2017)

pollutants completely and realize the regeneration of hydrogels after organic compound adsorption.

Hydrogel matrixes as chemical catalyst carriers

In order to promote the recovery of hydrogels after organic pollutant adsorption, the solvent extraction method is widely used, which may destroy the structure of hydrogels during the regeneration process and bring about secondary pollution. Advanced oxidation processes (AOPs) are promising technologies for the treatment of wastewater containing noneasily removable organic compounds, because they can effectively mineralize the contaminants or transform them into harmless products. By taking advantage of the mechanical property and oxidation property, some inorganic materials can be used in AOPs to remove organic pollutants completely. Hydrogels are not only ideal adsorbents for pollutant removal, but also suitable carriers for catalyst immobilization for providing hydrogels with catalytic performances.

Photocatalysis can not only remove the chemically stable and nonbiodegradable organic pollutants, but also efficiently degrade them under mild conditions. According to the summarized data provided in Table 4, the most commonly used photocatalyst is TiO_2. Hydrogels acted as matrixes to immobilize TiO_2 for photodegradation of pollutants such as MO (Badranova et al. 2016), MB (Mai et al. 2017), azo, anthraquinone (Dhanya and Aparna 2016), and 4-NP (Xia et al. 2019). Some hydrogels not only acted as matrixes for catalyst immobilization, but also could adsorb substrates first, and then take advantage of the synergistic effect between adsorption and catalysis. For example, some researchers entrapped TiO_2 into various hydrogels for adsorption and photodegradation of dyes such as reactive blue 4 (Yu et al. 2018b), RhB (Wang et al. 2018c), acid fuchsin (Zhou et al. 2017), Congo red (Thomas et al. 2016), and MB (Moon et al. 2013). Im et al. immobilized TiO_2 into PVA hydrogel by the electrospinning method for removing dyes (procion blue and acridine orange), and dyes were adsorbed first and then guided to the TiO_2 photocatalyst for degradation further (Im et al. 2010). Lučić et al. prepared the CS–TiO_2 hydrogel by immersing the CS hydrogel into TiO_2 NP solution for photodegrading dyes and found that the adsorption of dyes could be improved by increasing the amount of TiO_2 (Lučić et al. 2014). Apart from TiO_2, other photocatalysts are also applied. Xia et al. prepared SA–Ba hydrogel where Ba ion was used as both crosslinking agent and photocatalyst for degrading 4-NP (Xia et al. 2019). A simple chemical precipitation method was applied to load BiOI onto PHEA/APTM hydrogel to develop PHEA/APTM–BiOI to effectively eliminate methylparaben (MP) by visible light (Hu et al. 2019c). Zhu et al. introduced CdS into PHEA/poly(N-hydroxymethyl acrylamide) (PHEA/PHAM) by precipitation method and found that the swelling ratio and adsorption of BPA by PHEA/PHAM–CdS was higher than PHEA/PHAM, and showed the synergy between adsorption and photocatalytic oxidation (Zhu et al. 2018). Yang et al. reported that the adsorption capacity of SMZ by PHEA/PNMMA–CuS was higher than PHEA/PNMMA due to the presence of CuS which immobilized to PHEA/PNMMA by precipitation, and exhibited the synergy between adsorption and photocatalytic degradation (Yang et al. 2017). Hao et al. entrapped graphitic carbon nitride (g-C_3N_4) into PAM–bentonite hydrogel and found that the enhanced removal of total organic carbon (TOC) is attributed to the synergistic effect of adsorption and photocatalytic degradation (Hao et al. 2018). Mu et al. showed that BPA could be 100% removed in 12 min by the synergy of adsorption and photocatalysis using graphene hydrogel (rGH) which precipitated with Ag_3PO_4 (Mu et al. 2017). Kaur and Jindal entrapped zirconium (IV) in CS/gelatin hydrogel and the results showed that the adsorption and photodegradation of MB was enhanced compared with the pure CS/gelatin or zirconium (IV), showing the synergy between adsorption and photocatalytic degradation (Kaur and Jindal 2019). The addition of lanthanide into CS–graphite provided the hydrogel photocatalytic ability and increased the adsorption capacity for MB, as well as suppressed electron-hole recombination rates during the process of photocatalytic MB (Sirajudheen and Meenakshi 2019). Also, photocatalysts can be used as regeneration agent. For example, Chen et al. imbedded MoS into cellulose to prepare cellulose–MoS hydrogel, and the photoregeneration experiments after adsorption of MB showed that the adsorbent can be activated easily by illumination with little loss of dye adsorption capacity (Chen et al. 2017).

Recently, metal-binding hydrogels are applied as Fenton reagents because of the high metal-binding ability with hydrogels' abundant functional groups. Fe(II) was immobilized into CS/SA by Kang et al. via a simple crosslinking reaction to activate persulfate to degrade BPA. The CS/SA–Fe(II) system demonstrated a much higher removal efficiency of BPA (99.5%) than the conventional Fe(II) system (69.2%) with a negligible amount of Fe ions released into the solution, indicating that the CS/SA hydrogel played a positive role in protecting Fe(II) (Kang et al. 2018). Ben Hammouda et al. dropped SA solution into Fe(II) solution to prepare SA–Fe(II) composite for Fenton oxidation of indole, and the SA–Fe(II) catalyst present good stability and can be used for at least five times without an obvious decrease in activity (Ben Hammouda et al. 2016). Rashid et al. prepared CS–Cu–Fe complex by mixing CS powder, Fe(III), and Cu(II) together, and the mixture was precipitated by the addition of ethanol. The results indicated that discoloration of C.I. Reactive Black 5 by the hydrogel composite achieved 96.5% in a short reaction time, demonstrating the combination of adsorptive enrichment and catalytic degradation (Rashid et al. 2015). Zhang et al. immobilized Fe_2O_3 to rGO/polypyrrole (rGO/Ppy) by precipitation, and the rGO/Ppy–

Fe_2O_3 hydrogels could be easily separated via a magnet during Fenton degradation of MB, and showed superior reusability in recycling experiments (Zhang et al. 2017).

Hydrogel matrixes as enzyme carriers

Enzyme catalysis is another method to remove contaminants thoroughly, and it is more specific and mild than AOPs. But its application is challenged due to its unstable nature and low stability against variation in pH and temperature. Immobilization of enzyme is a widely used approach to enable repeated use and enhance the stability and durability of the enzyme which leads to economical operations.

Hydrogels can be applied as suitable carriers to restrict enzymes within the confined polymer spaces or networks (Falcone et al. 2019). Saoudi and Ghaouar entrapped laccase in PEGDA hydrogel, and the laccase kept 95% of its initial activity at 60 °C (Saoudi and Ghaouar 2019). Han et al. entrapped carbonic anhydrase, lysozyme, or xylanase in silk fibroi hydrogel and found that the three kinds of enzyme were increased in protein rigidity against pH denaturation (Han et al. 2018). Martín prepared SA/pectinase by entrapment, and the storage stability was improved (Martín et al. 2019). Olajuyigbe et al. entrapped laccase in SA for degradation of BPA, and the storage, pH, and temperature stability were slightly improved by immobilization (Olajuyigbe et al. 2019). Bilal et al. immobilized laccase in CS bead by crosslinking, and the immobilized biocatalyst showed good operational stability, retaining 71.24% of its original activity after 10 repeated catalytic cycles. Storage stability was improved also. In addition, the CS-based biocatalytic system achieved almost complete removal of BPA from the aqueous solution after 150 min of the transformation process (Bilal et al. 2019a).

Besides improved stability, reusability is another essential property for enzyme immobilization. PVA hydrogel protected protease from damage, helped maintain enzymatic activity at high levels, exhibited better reusability, and was easy to separate from the product (Zhang et al. 2018a). Naghdi et al. encapsulated laccase onto CS–biochar composite, with only 2% of laccase leaked during a 5-day period, and the encapsulated laccase exhibited 30% of the initial activity after five regeneration cycles (Naghdi et al. 2018). Sato et al. found that poly(ethylene glycol) methyl ether acrylate (PEGMEA)/lipase could catalyze the hydrolysis of triacetin without leakage of lipase or loss of activity during repeated use, and the efficiency was the same with free lipase (Sato et al. 2014). Bilal et al. entrapped horseradish peroxides in agarose/CS hydrogel, and 6-fold and 4-fold greater catalytic activity was achieved at 50 and 70 °C compared with free enzyme during dye degradation and the immobilized enzyme sustained above 90 and 60% of original activity after 5 and 10 continuous cycles of use (Bilal et al. 2019b). It can be concluded that immobilizing appropriate enzymes into hydrogels can catalyze target contaminants effectively and economically due to improved stability and reusability.

As has been discussed above (Table 5), entrapment is the commonly used approach for immobilizing enzymes into hydrogels, by which enzymes mixed with the aqueous monomer (or polymer) solution of hydrogels to obtain a homogeneous dispersion of enzymes throughout hydrogel networks. That is to say, enzyme immobilization is a one-step synthesis. Besides entrapment, hydrogels can be prepared first and then immobilize enzymes into solid hydrogels by adsorption or chemical crosslinking (Wolf and Paulino 2019). Liu et al. prepared cellulose–Fe_3O_4 hydrogel first and then papain was immobilized in it by adsorption, and the immobilized papain showed higher thermal stability than free papain (Liu et al. 2017). Liao et al. obtained chitin/PVA–Fe_3O_4/flavourzyme by immobilizing enzymes to solid hydrogels through adsorption and crosslinking, displaying preferable thermal stability and great reusability (Liao and Huang 2019a).

Challenges

Although hydrogels have exhibited superior performance in the adsorptive removal of a wide range of aqueous pollutants, including dyes, heavy metals, and ECs, their selective adsorption is rarely explored; thus, research efforts are needed to develop hydrogels with the desired structure and functionality possessing higher selectivity toward a specific pollutant. Many hydrogels have obtained satisfactory strength and adsorption property, but their chemical and biological stability needs to be taken into consideration in wastewater treatment for economic viability and sustainability, which are always ignored in the current research. In addition, although the smaller hydrogel particle size can improve the adsorption efficiency, the subsequent separation and recovery from the solution becomes a challenge. So how to reach a balance between the adsorption effect and their facility to recovery must be compromised.

Conclusion

This review has provided a general overview on hydrogel preparation and modification and the changes in mechanical strength, swelling ratio, and adsorption capacity of hydrogels due to the introduction of inorganic materials into networks, revealing that the hydrogel composites have better mechanical property and adsorption capacity compared with pure hydrogels. While a majority of studies have devoted to dye and metal adsorption by various hydrogels, there is clearly increased interest in EC removal afterwards. Moreover, hydrogels have potential applications in immobilizing

Table 5 Hydrogel matrixes as enzyme carriers

Hydrogel/enzyme	Immobilization methods	Surface chemistry	Properties	References
PEGDA/laccase	Entrapment	/	The laccase kept 95% of its initial activity at 60 °C in the hydrogel matrix.	Saoudi and Ghaouar (2019)
Cellulose–Fe_3O_4/papain	Adsorption	From FTIR, cellulose–Fe_3O_4/papain showed difference from the cellulose–Fe_3O_4 by the increase at the adsorption peak from 1000 to 1100 cm^{-1}, indicating the adsorption of the existing carboxyl and carboxylate in papain. And due to the nonuniform insertion of papain within the cellulose chains, the degree of crystallinity was lost a little.	Papain showed higher thermal stability than free enzyme.	Liu et al. (2017)
Chitin/PVA–Fe_3O_4/flavourzyme	Adsorption followed by crosslinking	/	The flavourzyme displayed preferable thermal stability and great reusability.	Liao and Huang (2019a)
Silk fibroi/enzyme (anhydrase or lysozyme or xylanase)	Entrapment	/	Entrapment of enzyme in hydrogel increased the protein rigidity against pH denaturation.	Han et al. (2018)
SA/pectinase	Entrapment	A strong and acute signal at 1720 cm^{-1} was observed by FTIR, which represented a spectral region associating to protein's structural components, particularly amide-I bands.	Storage stability was improved, and the values of k_m and V_{max} were similar with free enzyme.	Martín et al. (2019)
PVA–$Cu_3(PO_4)_2$•$3H_2O$/protease	Entrapment	/	The PVA hydrogel protected protease from damage, helped maintain enzymatic activity at high levels, and exhibited better reusability.	Zhang et al. (2018a)
CS–biochar/laccase	Entrapment	During the immobilization reaction, the impendent aldehyde groups on CS surface reacted with amino groups in Lac and form imino group (–CH=N–).	The encapsulated laccase exhibited 30% of the initial activity after 5 cycles toward the oxidation of ABTS and showed a moderate increase in enzyme stability against pH, temperature, and storage, with only 2% of laccase leaked during a 5-day period.	Naghdi et al. (2018)
PEGMEA/lipase	Entrapment	FITC-labeled lipase in pre-gel emulsion was clearly observed by photograph.	The immobilized lipase catalyzed the hydrolysis of triacetin without leakage of lipase or loss of activity during repeated use, and the efficiency was the same with free lipase.	Sato et al. (2014)
SA/laccase	Entrapment	/	The immobilized laccase was used for degradation of BPA, and the storage, pH, and temperature stability were slightly improved.	Olajuyigbe et al. (2019)
CS/laccase	Covalent	The laccase was covalently immobilized onto glutaraldehyde-activated CS beads, and the generation of aldehyde groups on the CS surface may react with the amino group of the laccase as well as other functional moieties (phenols, thiols, and imidazoles). The SEM observation revealed successful laccase immobilization with irregular aggregates on the CS surface.	The immobilized biocatalyst showed good operational stability and storage stability, and the CS-based biocatalytic system achieved almost complete removal of BPA from the aqueous solution after 150 min.	Bilal et al. (2019a)
Agarose/CS/horseradish peroxidase	Entrapment	SEM observation revealed that the surface of the polymer composite became rough after immobilization. FTIR analysis showed the appearance of an anti-parallel intermolecular β-sheet peak at 1633 cm^{-1}, which is attributed to the amide I of enzyme, indicating the aggregation of the protein at the p*D* values of 1.7 and 2.6.	The immobilized enzyme showed 6- and 4-fold greater catalytic activity at 50 and 70 °C compared with free enzyme and displayed insignificant loss in enzyme functionality sustaining above 90 and 60% of original activity after 5 and 10 continuous cycles of use for dye degradation.	Bilal et al. (2019b)

Note: "/" means surface chemistry was not mentioned in the reference

catalysts to removal of pollutants totally by the synergic function of adsorption and catalytic reaction, so hydrogel/catalyst composites should be developed as many as possible for reusability and sustainability concerns.

Funding information This work was supported by the Science and Technology Department of Siping City (2016053), the Department of Science and Technology of Jilin Province of China (20190303071SF, 20180520147JH), the Graduate Student Innovation and Entrepreneurship Competition of Jilin Normal University (201959), and the Innovation and Entrepreneurship Training Program for College Students of Jilin Province.

References

Abdollahi R, Taghizadeh MT, Savani S (2018) Thermal and mechanical properties of graphene oxide nanocomposite hydrogel based on poly (acrylic acid) grafted onto amylose. Polym Degrad Stab 147:151–158. https://doi.org/10.1016/j.polymdegradstab.2017.11.022

Afzal MZ, Sun XF, Liu J, Song C, Wang SG, Javed A (2018) Enhancement of ciprofloxacin sorption on chitosan/biochar hydrogel beads. Sci Total Environ 639:560–569. https://doi.org/10.1016/j.scitotenv.2018.05.129

Afzal MZ, Yue R, Sun XF, Song C, Wang SG (2019) Enhanced removal of ciprofloxacin using humic acid modified hydrogel beads. J Colloid Interface Sci 543:76–83. https://doi.org/10.1016/j.jcis.2019.01.083

Ahmad M, Zhang BL, Wang JQ, Xu J, Manzoor K, Ahmad S, Ikram S (2019) New method for hydrogel synthesis from diphenylcarbazide chitosan for selective copper removal. Int J Biol Macromol 136:189–198. https://doi.org/10.1016/j.ijbiomac.2019.06.084

Ai LH, Jiang J (2013) Catalytic reduction of 4-nitrophenol by silver nanoparticles stabilized on environmentally benign macroscopic biopolymer hydrogel. Bioresour Technol 132:374–377. https://doi.org/10.1016/j.biortech.2012.10.161

Alam A, Zhang Y, Kuan H-C, Lee S-H, Ma J (2018) Polymer composite hydrogels containing carbon nanomaterials—morphology and mechanical and functional performance. Prog Polym Sci 77:1–18. https://doi.org/10.1016/j.progpolymsci.2017.09.001

Aycan D, Alemdar N (2018) Development of pH-responsive chitosan-based hydrogel modified with bone ash for controlled release of amoxicillin. Carbohydr Polym 184:401–407. https://doi.org/10.1016/j.carbpol.2017.12.023

Badranova GU, Gotovtsev PM, Zubavichus YV, Staroselskiy IA, Vasiliev AL, Trunkin IN, Fedorov MV (2016) Biopolymer-based hydrogels for encapsulation of photocatalytic TiO_2 nanoparticles prepared by the freezing/thawing method. J Mol Liq 223:16–20. https://doi.org/10.1016/j.molliq.2016.07.135

Badsha MAH, Lo IMC (2019) An innovative pH-independent magnetically separable hydrogel for the removal of Cu(II) and Ni(II) ions from electroplating wastewater. J Hazard Mater. https://doi.org/10.1016/j.jhazmat.2019.121000

Baek J, Fan Y, Jeong S-H, Lee H-Y, Jung H-D, Kim H-E, Kim S, Jang T-S (2018) Facile strategy involving low-temperature chemical cross-linking to enhance the physical and biological properties of hyaluronic acid hydrogel. Carbohydr Polym 202:545–553. https://doi.org/10.1016/j.carbpol.2018.09.014

Balasubramanian R, Kim SS, Lee J, Lee J (2018) Effect of TiO_2 on highly elastic, stretchable UV protective nanocomposite films formed by using a combination of *k*-carrageenan, xanthan gum and gellan gum. Int J Biol Macromol 123:1020–1027. https://doi.org/10.1016/j.ijbiomac.2018.11.151

Ben Hammouda S, Adhoum N, Monser L (2016) Chemical oxidation of a malodorous compound, indole, using iron entrapped in calcium alginate beads. J Hazard Mater 301:350–361. https://doi.org/10.1016/j.jhazmat.2015.09.012

Benhalima T, Ferfera-Harrar H (2019) Eco-friendly porous carboxymethyl cellulose/dextran sulfate composite beads as reusable and efficient adsorbents of cationic dye methylene blue. Int J Biol Macromol 132:126–141. https://doi.org/10.1016/j.ijbiomac.2019.03.164

Bethi B, Manasa V, Srinija K, Sonawane SH (2018) Intensification of rhodamine-B dye removal using hydrodynamic cavitation coupled with hydrogel adsorption. Chem Eng Process 134:51–57. https://doi.org/10.1016/j.cep.2018.10.017

Bilal M, Jing Z, Zhao YP, Iqbal HMN (2019a) Immobilization of fungal laccase on glutaraldehyde cross-linked chitosan beads and its bio-catalytic potential to degrade bisphenol A. Biocatal Agric Biotechnol. https://doi.org/10.1016/j.bcab.2019.101174

Bilal M, Rasheed T, Zhao Y, Iqbal HMN (2019b) Agarose-chitosan hydrogel-immobilized horseradish peroxidase with sustainable bio-catalytic and dye degradation properties. Int J Biol Macromol 124:742–749. https://doi.org/10.1016/j.ijbiomac.2018.11.220

Bobula T, Buffa R, Hermannova M, Kohutova L, Prochazkova P, Vagnerova H, Cepa M, Wolfova L, Zidek O, Velebny V (2017) A novel photopolymerizable derivative of hyaluronan for designed hydrogel formation. Carbohydr Polym 161:277–285. https://doi.org/10.1016/j.carbpol.2017.01.009

Chen YC, Chen YH (2019) Thermo and pH-responsive methylcellulose and hydroxypropyl methylcellulose hydrogels containing K_2SO_4 for water retention and a controlled-release water-soluble fertilizer. Sci Total Environ 655:958–967. https://doi.org/10.1016/j.scitotenv.2018.11.264

Chen PP, Liu XY, Jin RD, Nie WY, Zhou YF (2017) Dye adsorption and photo-induced recycling of hydroxypropyl cellulose/molybdenum disulfide composite hydrogels. Carbohydr Polym 167:36–43. https://doi.org/10.1016/j.carbpol.2017.02.094

Chen X, Li PY, Kang Y, Zeng XT, Xie Y, Zhang YK, Wang YB, Xie T (2019) Preparation of temperature-sensitive xanthan/NIPA hydrogel using citric acid as crosslinking agent for bisphenol A adsorption. Carbohydr Polym 206:94–101. https://doi.org/10.1016/j.carbpol.2018.10.092

Dai HJ, Zhang YH, Ma L, Zhang H, Huang HH (2019) Synthesis and response of pineapple peel carboxymethyl cellulose-g-poly (acrylic acid-co-acrylamide)/graphene oxide hydrogels. Carbohydr Polym 215:366–376. https://doi.org/10.1016/j.carbpol.2019.03.090

Dargahi M, Ghasemzadeh H, Bakhtiary A (2018) Highly efficient absorption of cationic dyes by nano composite hydrogels based on *k*-carrageenan and nano silver chloride. Carbohydr Polym 181:587–595. https://doi.org/10.1016/j.carbpol.2017.11.108

Dehli F, Rebers L, Stubenrauch C, Southan A (2019) Highly ordered gelatin methacryloyl hydrogel foams with tunable pore size. Biomacromolecules 20:2666–2674. https://doi.org/10.1021/acs.biomac.9b00433

Dhanya A, Aparna K (2016) Synthesis and evaluation of TiO_2/chitosan based hydrogel for the adsorptional photocatalytic degradation of azo and anthraquinone dye under UV light irradiation. Procedia Technol 24:611–618. https://doi.org/10.1016/j.protcy.2016.05.141

Ding H, Liang X, Zhang XN, Wu ZL, Li Z, Sun G (2019) Tough supramolecular hydrogels with excellent self-recovery behavior mediated by metal-coordination interaction. Polymer 171:201–210. https://doi.org/10.1016/j.polymer.2019.03.061

Du HX, Piao MY (2018) Facile preparation of microscale hydrogel particles for high efficiency adsorption of bisphenol A from aqueous solution. Environ Sci Pollut Res 25:28562–28571. https://doi.org/10.1007/s11356-018-2879-0

Elbert DL (2011) Liquid-liquid two-phase systems for the production of porous hydrogels and hydrogel microspheres for biomedical applications: a tutorial review. Acta Biomater 7:31–56. https://doi.org/10.1016/j.actbio.2010.07.028

Elgarahy AM, Elwakeel KZ, Elshoubaky GA, Mohammad SH (2019) Untapped sepia shell–based composite for the sorption of cationic and anionic dyes. Water Air Soil Pollut:230. https://doi.org/10.1007/s11270-019-4247-1

Emami Z, Ehsani M, Zandi M, Foudazi R (2018) Controlling alginate oxidation conditions for making alginate-gelatin hydrogels. Carbohydr Polym 198:509–517. https://doi.org/10.1016/j.carbpol.2018.06.080

Erfkamp J, Guenther M, Gerlach G (2019) Enzyme-functionalized piezoresistive hydrogel biosensors for the detection of urea. Sensors (Basel):19. https://doi.org/10.3390/s19132858

Falcone N, Shao T, Rashid R, Kraatz HB (2019) Enzyme entrapment in amphiphilic myristyl-phenylalanine hydrogels. Molecules. https://doi.org/10.3390/molecules24162884

Fan L, Lu Y, Yang LY, Huang F, Ouyang XK (2019) Fabrication of polyethylenimine-functionalized sodium alginate/cellulose nanocrystal/polyvinyl alcohol core-shell microspheres ((PVA/SA/CNC)@PEI) for diclofenac sodium adsorption. J Colloid Interface Sci 554:48–58. https://doi.org/10.1016/j.jcis.2019.06.099

Genevro GM, de Moraes MA, Beppu MM (2019) Freezing influence on physical properties of glucomannan hydrogels. Int J Biol Macromol 128:401–405. https://doi.org/10.1016/j.ijbiomac.2019.01.112

Geng HJ (2018) Preparation and characterization of cellulose/N,N'-methylene bisacrylamide/graphene oxide hybrid hydrogels and aerogels. Carbohydr Polym 196:289–298. https://doi.org/10.1016/j.carbpol.2018.05.058

Getachew BA, Guo W, Zhong M, Kim J-H (2019) Asymmetric hydrogel-composite membranes with improved water permeability and self-healing property. J Membr Sci 578:196–202. https://doi.org/10.1016/j.memsci.2019.01.022

Gholamhoseini M, Habibzadeh F, Ataei R, Hemmati P, Ebrahimian E (2018) Zeolite and hydrogel improve yield of greenhouse cucumber in soil-less medium under water limitation. Rhizosphere 6:7–10. https://doi.org/10.1016/j.rhisph.2018.01.006

Glass S, Trinklein B, Abel B, Schulze A (2018) TiO_2 as photosensitizer and photoinitiator for synthesis of photoactive TiO_2-PEGDA hydrogel without organic photoinitiator. Front Chem 6:340–349. https://doi.org/10.3389/fchem.2018.00340

Godiya CB, Cheng X, Li D, Chen Z, Lu X (2018) Carboxymethyl cellulose/polyacrylamide composite hydrogel for cascaded treatment/reuse of heavy metal ions in wastewater. J Hazard Mater 364:28–38. https://doi.org/10.1016/j.jhazmat.2018.09.076

Godiya CB, Liang M, Sayed SM, Li D, Lu X (2019) Novel alginate/polyethyleneimine hydrogel adsorbent for cascaded removal and utilization of Cu^{2+} and Pb^{2+} ions. J Environ Manag 232:829–841. https://doi.org/10.1016/j.jenvman.2018.11.131

Gogoi N, Barooah M, Majumdar G, Chowdhury D (2015) Carbon dots rooted agarose hydrogel hybrid platform for optical detection and separation of heavy metal ions. ACS Appl Mater Interfaces 7:3058–3067. https://doi.org/10.1021/am506558d

Goh PS, Naim R, Rahbari-Sisakht M, Ismail AF (2019) Modification of membrane hydrophobicity in membrane contactors for environmental remediation. Sep Purif Technol. https://doi.org/10.1016/j.seppur.2019.115721

Gonzalez K, Garcia-Astrain C, Santamaria-Echart A, Ugarte L, Averous L, Eceiza A, Gabilondo N (2018) Starch/graphene hydrogels via click chemistry with relevant electrical and antibacterial properties. Carbohydr Polym 202:372–381. https://doi.org/10.1016/j.carbpol.2018.09.007

Hafezi Moghaddam R, Haji Shabani AM, Dadfarnia S (2019) Synthesis of new hydrogels based on pectin by electron beam irradiation with and without surface modification for methylene blue removal. J Environ Chem Eng. https://doi.org/10.1016/j.jece.2019.102919

Hai TN (2016) Comments on "Effect of temperature on the adsorption of methylene blue dye onto sulfuric acid–treated orange peel". Chem Eng Commun 204:134–139. https://doi.org/10.1080/00986445.2016.1245185

Han YY, Wu XD, Zhang XX, Zhou ZH, Lu CH (2016) Reductant-free synthesis of silver nanoparticles-doped cellulose microgels for catalyzing and product separation. ACS Sustain Chem Eng 4:6322–6331. https://doi.org/10.1021/acssuschemeng.6b00889

Han YY, Yu SH, Liu LC, Zhao SJ, Yang TX, Yang YJ, Fang YM, Lv SS (2018) Silk fibroin-based hydrogels as a protective matrix for stabilization of enzymes against pH denaturation. Mol Catal 457:24–32. https://doi.org/10.1016/j.mcat.2018.07.009

Hao Q, Chen T, Wang RT, Feng JR, Chen DM, Yao WQ (2018) A separation-free polyacrylamide/bentonite/graphitic carbon nitride hydrogel with excellent performance in water treatment. J Clean Prod 197:1222–1230. https://doi.org/10.1016/j.jclepro.2018.06.289

Heimbuck AM, Priddy-Arrington TR, Sawyer BJ, Caldorera-Moore ME (2019) Effects of post-processing methods on chitosan-genipin hydrogel properties. Mater Sci Eng C Mater Biol Appl 98:612–618. https://doi.org/10.1016/j.msec.2018.12.119

Hu X, Wang Y, Xu M, Zhang L, Zhang J, Dong W (2018) Mechanical testing and reinforcing mechanisms of a magnetic field-sensitive hydrogel prepared by microwave-assisted polymerization. Polym Test 71:344–351. https://doi.org/10.1016/j.polymertesting.2018.09.027

Hu XS, Liang R, Li J, Liu ZP, Sun GX (2019a) Mechanically strong hydrogels achieved by designing homogeneous network structure. Mater Des. https://doi.org/10.1016/j.matdes.2018.107547

Hu XY, Wang YM, Xu M, Zhang LL, Zhang JF, Dong W (2019b) Development of photocrosslinked salecan composite hydrogel embedding titanium carbide nanoparticles as cell scaffold. Int J Biol Macromol 123:549–557. https://doi.org/10.1016/j.ijbiomac.2018.11.125

Hu YY, Li ZK, Yang JH, Zhu HJ (2019c) Degradation of methylparaben using BiOI-hydrogel composites activated peroxymonosulfate under visible light irradiation. Chem Eng J 360:200–211. https://doi.org/10.1016/j.cej.2018.11.217

Huang B, Liu MX, Long ZR, Shen Y, Zhou CR (2017) Effects of halloysite nanotubes on physical properties and cytocompatibility of alginate composite hydrogels. Mater Sci Eng C Mater Biol Appl 70:303–310. https://doi.org/10.1016/j.msec.2016.09.001

Huang S, Zhao Z, Feng C, Mayes E, Yang J (2018a) Nanocellulose reinforced P(AAm-co-AAc) hydrogels with improved mechanical properties and biocompatibility. Compos Part A Appl Sci 112:395–404. https://doi.org/10.1016/j.compositesa.2018.06.028

Huang YW, Zeng M, Chen JB, Wang YQ, Xu QY (2018b) Multi-structural network design and mechanical properties of graphene oxide filled chitosan-based hydrogel nanocomposites. Mater Des 148:104–114. https://doi.org/10.1016/j.matdes.2018.03.055

Ilgin P, Ozay O, Ozay H (2019) A novel hydrogel containing thioether group as selective support material for preparation of gold nanoparticles: synthesis and catalytic applications. Appl Catal B Environ 241:415–423. https://doi.org/10.1016/j.apcatb.2018.09.066

Im JS, Bai BC, In SJ, Lee YS (2010) Improved photodegradation properties and kinetic models of a solar-light-responsive photocatalyst when incorporated into electrospun hydrogel fibers. J Colloid Interface Sci 346:216–221. https://doi.org/10.1016/j.jcis.2010.02.043

Jiang HC, Duan LJ, Ren XY, Gao GH (2019) Hydrophobic association hydrogels with excellent mechanical and self-healing properties. Eur Polym J 112:660–669. https://doi.org/10.1016/j.eurpolymj.2018.10.031

Jung HS, Kim HC, Ho Park W (2019) Robust methylcellulose hydrogels reinforced with chitin nanocrystals. Carbohydr Polym 213:311–319. https://doi.org/10.1016/j.carbpol.2019.03.009

Kandile NG, Mohamed HM (2019) Chitosan nanoparticle hydrogel based sebacoyl moiety with remarkable capability for metal ion removal from aqueous systems. Int J Biol Macromol 122:578–586. https://doi.org/10.1016/j.ijbiomac.2018.10.198

Kang WT, Bi B, Zhuo RX, Jiang XL (2017) Photocrosslinked methacrylated carboxymethyl chitin hydrogels with tunable

degradation and mechanical behavior. Carbohydr Polym 160:18–25. https://doi.org/10.1016/j.carbpol.2016.12.032

Kang Y-G, Vu HC, Le TT, Chang Y-S (2018) Activation of persulfate by a novel Fe(II)-immobilized chitosan/alginate composite for bisphenol A degradation. Chem Eng J 353:736–745. https://doi.org/10.1016/j.cej.2018.07.175

Kang SC, Qin L, Zhao YL, Wang W, Zhang TT, Yang L, Rao F, Song SX (2019) Enhanced removal of methyl orange on exfoliated montmorillonite/chitosan gel in presence of methylene blue. Chemosphere. https://doi.org/10.1016/j.chemosphere.2019.124693

Kangwansupamonkon W, Klaikaew N, Kiatkamjornwong S (2018) Green synthesis of titanium dioxide/acrylamide-based hydrogel composite, self degradation and environmental applications. Eur Polym J 107:118–131. https://doi.org/10.1016/j.eurpolymj.2018.08.004

Karbarz M, Khalil AM, Wolowicz K, Kaniewska K, Romanski J, Stojek Z (2018) Efficient removal of cadmium and lead ions from water by hydrogels modified with cystine. J Environ Chem Eng 6:3962–3970. https://doi.org/10.1016/j.jece.2018.05.054

Kaur K, Jindal R (2019) Comparative study on the behaviour of chitosan-gelatin based hydrogel and nanocomposite ion exchanger synthesized under microwave conditions towards photocatalytic removal of cationic dyes. Carbohydr Polym 207:398–410. https://doi.org/10.1016/j.carbpol.2018.12.002

Khan M, Lo IMC (2016) A holistic review of hydrogel applications in the adsorptive removal of aqueous pollutants: recent progress, challenges, and perspectives. Water Res 106:259–271. https://doi.org/10.1016/j.watres.2016.10.008

Khan M, Lo IMC (2017) Removal of ionizable aromatic pollutants from contaminated water using nano γ-Fe_2O_3 based magnetic cationic hydrogel: sorptive performance, magnetic separation and reusability. J Hazard Mater 322:195–204. https://doi.org/10.1016/j.jhazmat.2016.01.051

Kim HH, Kim JW, Choi J, Park YH, Ki CS (2018) Characterization of silk hydrogel formed with hydrolyzed silk fibroin-methacrylate via photopolymerization. Polymer 153:232–240. https://doi.org/10.1016/j.polymer.2018.08.019

Kiruba UP, Kumar PS, Prabhakaran C, Aditya V (2014) Characteristics of thermodynamic, isotherm, kinetic, mechanism and design equations for the analysis of adsorption in Cd(II) ions-surface modified Eucalyptus seeds system. J Taiwan Inst Chem E 45:2957–2968. https://doi.org/10.1016/j.jtice.2014.08.016

Kishore PVN, Shankar MS, Satyanarayana M (2017) Detection of trace amounts of chromium(VI) using hydrogel coated fiber Bragg grating. Sensors Actuators B Chem 243:626–633. https://doi.org/10.1016/j.snb.2016.12.017

Kluczka J, Gnus M, Kazek-Kęsik A, Dudek G (2018) Zirconium-chitosan hydrogel beads for removal of boron from aqueous solutions. Polymer 150:109–118. https://doi.org/10.1016/j.polymer.2018.07.010

Kong WJ, Yue QY, Li Q, Gao BY (2019a) Adsorption of Cd^{2+} on GO/PAA hydrogel and preliminary recycle to GO/PAA-CdS as efficient photocatalyst. Sci Total Environ 668:1165–1174. https://doi.org/10.1016/j.scitotenv.2019.03.095

Kong Y, Zhuang Y, Han ZY, Yu JW, Shi BY, Han K, Hao HT (2019b) Dye removal by eco-friendly physically cross-linked double network polymer hydrogel beads and their functionalized composites. J Environ Sci (China) 78:81–91. https://doi.org/10.1016/j.jes.2018.07.006

Kumar A, Zo SM, Kim JH, Kim S-C, Han SS (2019) Enhanced physical, mechanical, and cytocompatibility behavior of polyelectrolyte complex hydrogels by reinforcing halloysite nanotubes and graphene oxide. Compos Sci Technol 175:35–45. https://doi.org/10.1016/j.compscitech.2019.03.008

Lee C, Pant B, Kim B-S, Jang R-S, Park S, Park M, Park S-J, Kim H-Y (2017) Carbon quantum dots incorporated keratin/polyvinyl alcohol hydrogels: preparation and photoluminescent assessment. Mater Lett 207:57–61. https://doi.org/10.1016/j.matlet.2017.07.058

Lee HY, Hwang CH, Kim HE, Jeong SH (2018) Enhancement of biostability and mechanical properties of hyaluronic acid hydrogels by tannic acid treatment. Carbohydr Polym 186:290–298. https://doi.org/10.1016/j.carbpol.2018.01.056

Lengert E, Kozlova A, Pavlov AM, Atkin V, Verkhovskii R, Kamyshinsky R, Demina P, Vasiliev AL, Venig SB, Bukreeva TV (2019) Novel type of hollow hydrogel microspheres with magnetite and silver nanoparticles. Mater Sci Eng C Mater Biol Appl 98:1114–1121. https://doi.org/10.1016/j.msec.2019.01.030

Li P, Zhao J, Chen Y, Cheng B, Yu Z, Zhao Y, Yan XT, Tong ZR, Jin SH (2017) Preparation and characterization of chitosan physical hydrogels with enhanced mechanical and antibacterial properties. Carbohydr Polym 157:1383–1392. https://doi.org/10.1016/j.carbpol.2016.11.016

Li R, Lin J, Fang Y, Yu C, Zhang JJ, Xue YM, Liu ZY, Zhang J, Tang CC, Huang Y (2018) Porous boron nitride nanofibers/PVA hydrogels with improved mechanical property and thermal stability. Ceram Int 44:22439–22444. https://doi.org/10.1016/j.ceramint.2018.09.011

Li M, Jiang XX, Wang D, Xu ZY, Yang MH (2019) In situ reduction of silver nanoparticles in the lignin based hydrogel for enhanced antibacterial application. Colloids Surf B: Biointerfaces 177:370–376. https://doi.org/10.1016/j.colsurfb.2019.02.029

Liang XX, Omer AM, Hu ZH, Wang YG, Yu D, Ouyang XK (2019a) Efficient adsorption of diclofenac sodium from aqueous solutions using magnetic amine-functionalized chitosan. Chemosphere 217:270–278. https://doi.org/10.1016/j.chemosphere.2018.11.023

Liang XX, Ouyang XK, Wang S, Yang LY, Huang F, Ji C, Chen X (2019b) Efficient adsorption of Pb(II) from aqueous solutions using aminopropyltriethoxysilane-modified magnetic attapulgite@chitosan (APTS-Fe_3O_4/APT@CS) composite hydrogel beads. Int J Biol Macromol 137:741–750. https://doi.org/10.1016/j.ijbiomac.2019.06.244

Liao J, Huang HH (2019a) Green magnetic hydrogels synthesis, characterization and flavourzyme immobilization based on chitin from *Hericium erinaceus* residue and polyvinyl alcohol. Int J Biol Macromol 138:462–472. https://doi.org/10.1016/j.ijbiomac.2019.07.038

Liao J, Huang HH (2019b) Magnetic chitin hydrogels prepared from *Hericium erinaceus* residues with tunable characteristics: a novel biosorbent for Cu^{2+} removal. Carbohydr Polym 220:191–201. https://doi.org/10.1016/j.carbpol.2019.05.074

Liao CA, Wu Q, Su T, Zhang D, Wu QS, Wang QG (2014) Nanocomposite gels via in situ photoinitiation and disassembly of TiO_2-clay composites with polymers applied as UV protective films. ACS Appl Mater Interfaces 6:1356–1360. https://doi.org/10.1021/am404515b

Lin FC, Zheng RT, Chen JW, Su WM, Dong BY, Lin CS, Huang B, Lu BL (2019a) Microfibrillated cellulose enhancement to mechanical and conductive properties of biocompatible hydrogels. Carbohydr Polym 205:244–254. https://doi.org/10.1016/j.carbpol.2018.10.037

Lin Q, Wu YY, Jiang X, Lin FC, Liu X, Lu BL (2019b) Removal of bisphenol A from aqueous solution via host-guest interactions based on beta-cyclodextrin grafted cellulose bead. Int J Biol Macromol 140:1–9. https://doi.org/10.1016/j.ijbiomac.2019.08.116

Liu AL, Garcia AJ (2016) Methods for generating hydrogel particles for protein delivery. Ann Biomed Eng 44:1946–1958. https://doi.org/10.1007/s10439-016-1637-z

Liu ZJ, Li DX, Dai HJ, Huang HH (2017) Preparation and characterization of papain embedded in magnetic cellulose hydrogels prepared from tea residue. J Mol Liq 232:449–456. https://doi.org/10.1016/j.molliq.2017.02.100

Liu CY, Liu HY, Xiong TH, Xu AR, Pan BL, Tang KY (2018a) Graphene oxide reinforced alginate/PVA double network hydrogels for

efficient dye removal. Polymers (Basel). https://doi.org/10.3390/polym10080835
Liu FG, Li RR, Mao LK, Gao YX (2018b) Ethanol-induced composite hydrogel based on propylene glycol alginate and zein: formation, characterization and application. Food Chem 255:390–398. https://doi.org/10.1016/j.foodchem.2018.02.072
Liu NB, Chen JM, Zhuang J, Zhu P (2018c) Fabrication of engineered nanoparticles on biological macromolecular (PEGylated chitosan) composite for bio-active hydrogel system in cardiac repair applications. Int J Biol Macromol 117:553–558. https://doi.org/10.1016/j.ijbiomac.2018.04.196
Liu CG, Zheng WC, Xie RX, Liu YP, Liang Z, Luo GA, Ding MY, Liang QL (2019a) Microfluidic fabrication of water-in-water droplets encapsulated in hydrogel microfibers. Chin Chem Lett 30:457–460. https://doi.org/10.1016/j.cclet.2018.09.010
Liu XW, Luan S, Li W (2019b) Utilization of waste hemicelluloses lye for superabsorbent hydrogel synthesis. Int J Biol Macromol 132:954–962. https://doi.org/10.1016/j.ijbiomac.2019.04.041
Liu XX, Chang MM, He B, Meng L, Wang XH, Sun RC, Ren JL, Kong FG (2019c) A one-pot strategy for preparation of high-strength carboxymethyl xylan-g-poly(acrylic acid) hydrogels with shape memory property. J Colloid Interface Sci 538:507–518. https://doi.org/10.1016/j.jcis.2018.12.023
Liu YZ, Tottori N, Nisisako T (2019d) Microfluidic synthesis of highly spherical calcium alginate hydrogels based on external gelation using an emulsion reactant. Sensors Actuators B Chem 283:802–809. https://doi.org/10.1016/j.snb.2018.12.101
Long L, Hu XL, Yan JP, Zeng YF, Zhang JQ, Xue YW (2019) Novel chitosan-ethylene glycol hydrogel for the removal of aqueous perfluorooctanoic acid. J Environ Sci (China) 84:21–28. https://doi.org/10.1016/j.jes.2019.04.007
Lučić M, Milosavljević N, Radetić M, Šaponjić Z, Radoičić M, Kalagasidis Krušić M (2014) The potential application of TiO_2/hydrogel nanocomposite for removal of various textile azo dyes. Sep Purif Technol 122:206–216. https://doi.org/10.1016/j.seppur.2013.11.002
Luo ZF, Chen HY, Wu SC, Yang C, Cheng JH (2019) Enhanced removal of bisphenol A from aqueous solution by aluminum-based MOF/sodium alginate-chitosan composite beads. Chemosphere. https://doi.org/10.1016/j.chemosphere.2019.124493
Ma CX, Gao JX, Wang D, Yuan YH, Wen J, Yan BJ, Zhao SL, Zhao XM, Sun Y, Wang XL, Wang N (2019) Sunlight polymerization of poly(amidoxime) hydrogel membrane for enhanced uranium extraction from seawater. Adv Sci (Weinh). https://doi.org/10.1002/advs.201900085
Mahinroosta M, Jomeh Farsangi Z, Allahverdi A, Shakoori Z (2018) Hydrogels as intelligent materials: a brief review of synthesis, properties and applications. Mater Today Chem 8:42–55. https://doi.org/10.1016/j.mtchem.2018.02.004
Mai NXD, Bae J, Kim IT, Park SH, Lee G-W, Kim JH, Lee D, Son HB, Lee Y-C, Hur J (2017) A recyclable, recoverable, and reformable hydrogel-based smart photocatalyst. Environ Sci Nano 4:955–966. https://doi.org/10.1039/c6en00695g
Makhado E, Pandey S, Nomngongo PN, Ramontja J (2018) Preparation and characterization of xanthan gum-cl-poly(acrylic acid)/o-MWCNTs hydrogel nanocomposite as highly effective re-usable adsorbent for removal of methylene blue from aqueous solutions. J Colloid Interface Sci 513:700–714. https://doi.org/10.1016/j.jcis.2017.11.060
Mamaghani KR, Naghib SM, Zahedi A, Rahmanian M, Mozafari M (2018) GelMa/PEGDA containing graphene oxide as an IPN hydrogel with superior mechanical performance. Mater Today Proc 5:15790–15799. https://doi.org/10.1016/j.matpr.2018.04.193
Martin N, Youssef G (2018) Dynamic properties of hydrogels and fiber-reinforced hydrogels. J Mech Behav Biomed Mater 85:194–200. https://doi.org/10.1016/j.jmbbm.2018.06.008
Martín MC, López OV, Ciolino AE, Morata VI, Villar MA, Ninago MD (2019) Immobilization of enological pectinase in calcium alginate hydrogels: a potential biocatalyst for winemaking. Biocatal Agric Biotechnol. https://doi.org/10.1016/j.bcab.2019.101091
Martínez MV, Rivarola CR, Miras MC, Barbero CA (2017) A colorimetric iron sensor based on the partition of phenanthroline complexes into polymeric hydrogels. Combinatorial synthesis and high throughput screening of the hydrogel matrix. Sensors Actuators B Chem 241:19–32. https://doi.org/10.1016/j.snb.2016.10.013
Meng Y, Li CX, Liu XQ, Lu J, Cheng Y, Xiao LP, Wang HS (2019) Preparation of magnetic hydrogel microspheres of lignin derivate for application in water. Sci Total Environ 685:847–855. https://doi.org/10.1016/j.scitotenv.2019.06.278
Mirabedini M, Kassaee MZ, Poorsadeghi S (2016) Novel magnetic chitosan hydrogel film, cross-linked with glyoxal as an efficient adsorbent for removal of toxic Cr(VI) from water. Arab J Sci Eng 42:115–124. https://doi.org/10.1007/s13369-016-2062-1
Mohammadian M, Sahraei R, Ghaemy M (2019) Synthesis and fabrication of antibacterial hydrogel beads based on modified-gum tragacanth/poly(vinyl alcohol)/Ag^0 highly efficient sorbent for hard water softening. Chemosphere 225:259–269. https://doi.org/10.1016/j.chemosphere.2019.03.040
Mohammadinezhad A, Marandi GB, Farsadrooh M, Javadian H (2017) Synthesis of poly(acrylamide-co-itaconic acid)/MWCNTs superabsorbent hydrogel nanocomposite by ultrasound-assisted technique: swelling behavior and Pb (II) adsorption capacity. Ultrason Sonochem. https://doi.org/10.1016/j.ultsonch.2017.12.028
Montaser AS, Wassel AR, Al-Shaye'a ON (2018) Synthesis, characterization and antimicrobial activity of Schiff bases from chitosan and salicylaldehyde/TiO_2 nanocomposite membrane. Int J Biol Macromol 124:802–809. https://doi.org/10.1016/j.ijbiomac.2018.11.229
Moon Y-E, Jung G, Yun J, Kim H-I (2013) Poly(vinyl alcohol)/poly(-acrylic acid)/TiO_2/graphene oxide nanocomposite hydrogels for pH-sensitive photocatalytic degradation of organic pollutants. Mater Sci Eng B 178:1097–1103. https://doi.org/10.1016/j.mseb.2013.07.002
Mu CF, Zhang Y, Cui WQ, Liang YH, Zhu YF (2017) Removal of bisphenol A over a separation free 3D Ag_3PO_4-graphene hydrogel via an adsorption-photocatalysis synergy. Appl Catal B Environ 212:41–49. https://doi.org/10.1016/j.apcatb.2017.04.018
Naghdi M, Taheran M, Brar SK, Kermanshahi-Pour A, Verma M, Surampalli RY (2018) Fabrication of nanobiocatalyst using encapsulated laccase onto chitosan-nanobiochar composite. Int J Biol Macromol 124:530–536. https://doi.org/10.1016/j.ijbiomac.2018.11.234
Nam J, Jung I-B, Kim B, Lee S-M, Kim S-E, Lee K-N, Shin D-S (2018) A colorimetric hydrogel biosensor for rapid detection of nitrite ions. Sensors Actuators B Chem 270:112–118. https://doi.org/10.1016/j.snb.2018.04.171
Namazi H, Hasani M, Yadollahi M (2019) Antibacterial oxidized starch/ZnO nanocomposite hydrogel: synthesis and evaluation of its swelling behaviours in various pHs and salt solutions. Int J Biol Macromol 126:578–584. https://doi.org/10.1016/j.ijbiomac.2018.12.242
Natkański P, Kuśtrowski P, Białas A, Wach A, Rokicińska A, Kozak M, Lityńska-Dobrzyńska L (2016) Hydrogel template-assisted synthesis of nanometric Fe_2O_3 supported on exfoliated clay. Microporous Mesoporous Mater 221:212–219. https://doi.org/10.1016/j.micromeso.2015.09.047
Neeraj G, Krishnan S, Senthil Kumar P, Shriaishvarya KR, Vinoth Kumar V (2016) Performance study on sequestration of copper ions from contaminated water using newly synthesized high effective chitosan coated magnetic nanoparticles. J Mol Liq 214:335–346. https://doi.org/10.1016/j.molliq.2015.11.051
Nešović K, Janković A, Kojić V, Vukašinović-Sekulić M, Perić-Grujić A, Rhee KY, Mišković-Stanković V (2018) Silver/poly(vinyl alcohol)/

chitosan/graphene hydrogels—synthesis, biological and physicochemical properties and silver release kinetics. Compos Part B Eng 154:175–185. https://doi.org/10.1016/j.compositesb.2018.08.005

Nguyen N-T, Liu J-H (2014) A green method for in situ synthesis of poly(vinyl alcohol)/chitosan hydrogel thin films with entrapped silver nanoparticles. J Taiwan Inst Chem E 45:2827–2833. https://doi.org/10.1016/j.jtice.2014.06.017

Ohemeng-Boahen G, Sewu DD, Woo SH (2019) Preparation and characterization of alginate-kelp biochar composite hydrogel bead for dye removal. Environ Sci Pollut Res Int. https://doi.org/10.1007/s11356-019-06421-2

Ojeda M, Chen BB, Leung DYC, Xuan J, Wang HZ (2017) A hydrogel template synthesis of TiO_2 nanoparticles for aluminium-ion batteries. Energy Procedia 105:3997–4002. https://doi.org/10.1016/j.egypro.2017.03.836

Olajuyigbe FM, Adetuyi OY, Fatokun CO (2019) Characterization of free and immobilized laccase from *Cyberlindnera fabianii* and application in degradation of bisphenol A. Int J Biol Macromol 125:856–864. https://doi.org/10.1016/j.ijbiomac.2018.12.106

Panão CO, Campos ELS, Lima HHC, Rinaldi AW, Lima-Tenório MK, Tenório-Neto ET, Guilherme MR, Asefa T, Rubira AF (2019) Ultra-absorbent hybrid hydrogel based on alginate and SiO_2 microspheres: a high-water-content system for removal of methylene blue. J Mol Liq 276:204–213. https://doi.org/10.1016/j.molliq.2018.11.157

Pathak SK, Dwivedi C, Banerjee C, Singh KK, Tripathi SC, Kumar M, Gandhi PM (2016) Potassium zinc hexacyanoferrate encapsulated hydro-gel beads for removal of radio-cesium. Asian J Mater Chem 1:14–20. https://doi.org/10.14233/ajmc.2016.AJMC-P3

Peng N, Hu DN, Zeng J, Li Y, Liang L, Chang CY (2016) Superabsorbent cellulose–clay nanocomposite hydrogels for highly efficient removal of dye in water. ACS Sustain Chem Eng 4:7217–7224. https://doi.org/10.1021/acssuschemeng.6b02178

Pettinelli N, Rodriguez-Llamazares S, Abella V, Barral L, Bouza R, Farrag Y, Lago F (2019) Entrapment of chitosan, pectin or kappa-carrageenan within methacrylate based hydrogels: effect on swelling and mechanical properties. Mater Sci Eng C Mater Biol Appl 96:583–590. https://doi.org/10.1016/j.msec.2018.11.071

Piao YZ, Chen BQ (2017) Synthesis and mechanical properties of double cross-linked gelatin-graphene oxide hydrogels. Int J Biol Macromol 101:791–798. https://doi.org/10.1016/j.ijbiomac.2017.03.155

Pourbeyram S, Mohammadi S (2014) Synthesis and characterization of highly stable and water dispersible hydrogel–copper nanocomposite. J Non-Cryst Solids 402:58–63. https://doi.org/10.1016/j.jnoncrysol.2014.05.020

Pourjavadi A, Tehrani ZM, Salimi H, Banazadeh A, Abedini N (2015) Hydrogel nanocomposite based on chitosan-g-acrylic acid and modified nanosilica with high adsorption capacity for heavy metal ion removal. Iran Polym J 24:725–734. https://doi.org/10.1007/s13726-015-0360-1

Pourjavadi A, Doroudian M, Ahadpour A, Azari S (2019) Injectable chitosan/k-carrageenan hydrogel designed with Au nanoparticles: a conductive scaffold for tissue engineering demands. Int J Biol Macromol 126:310–317. https://doi.org/10.1016/j.ijbiomac.2018.11.256

Qi X, Wu L, Su T, Zhang J, Dong W (2018) Polysaccharide-based cationic hydrogels for dye adsorption. Colloids Surf B: Biointerfaces 170:364–372. https://doi.org/10.1016/j.colsurfb.2018.06.036

Qi XL, Li ZP, Shen LL, Qin T, Qian Y, Zhao SZ, Liu MC, Zeng QK, Shen JL (2019a) Highly efficient dye decontamination via microbial salecan polysaccharide-based gels. Carbohydr Polym 219:1–11. https://doi.org/10.1016/j.carbpol.2019.05.021

Qi XL, Liu RN, Chen MY, Li ZP, Qin T, Qian YN, Zhao SZ, Liu MC, Zeng QK, Shen J (2019b) Removal of copper ions from water using polysaccharide-constructed hydrogels. Carbohydr Polym 209:101–110. https://doi.org/10.1016/j.carbpol.2019.01.015

Qin H, Wang J, Wang T, Gao XM, Wan QB, Pei XB (2018) Preparation and characterization of chitosan/β-glycerophosphate thermal-sensitive hydrogel reinforced by graphene oxide. Front Chem 6:565–576. https://doi.org/10.3389/fchem.2018.00565

Ramos MLP, González JA, Albornoz SG, Pérez CJ, Villanueva ME, Giorgieri SA, Copello GJ (2016) Chitin hydrogel reinforced with TiO_2 nanoparticles as an arsenic sorbent. Chem Eng J 285:581–587. https://doi.org/10.1016/j.cej.2015.10.035

Rao Z, Liu S, Wu R, Wang G, Sun Z, Bai L, Wang W, Chen H, Yang H, Wei D, Niu Y (2019) Fabrication of dual network self-healing alginate/guar gum hydrogels based on polydopamine-type microcapsules from mesoporous silica nanoparticles. Int J Biol Macromol 129:916–926. https://doi.org/10.1016/j.ijbiomac.2019.02.089

Rashid S, Shen CS, Chen XG, Li S, Chen YH, Wen YZ, Liu JS (2015) Enhanced catalytic ability of chitosan–Cu–Fe bimetal complex for the removal of dyes in aqueous solution. RSC Adv 5:90731–90741. https://doi.org/10.1039/c5ra14711e

Rassu G, Salis A, Porcu EP, Giunchedi P, Roldo M, Gavini E (2016) Composite chitosan/alginate hydrogel for controlled release of deferoxamine: a system to potentially treat iron dysregulation diseases. Carbohydr Polym 136:1338–1347. https://doi.org/10.1016/j.carbpol.2015.10.048

Raval HD, Rana PS, Maiti S (2015) A novel high-flux, thin-film composite reverse osmosis membrane modified by chitosan for advanced water treatment. RSC Adv 5:6687–6694. https://doi.org/10.1039/c4ra12610f

Ren LL, Xu J, Zhang YC, Zhou J, Chen DH, Chang ZY (2019) Preparation and characterization of porous chitosan microspheres and adsorption performance for hexavalent chromium. Int J Biol Macromol 135:898–906. https://doi.org/10.1016/j.ijbiomac.2019.06.007

Rotbaum Y, Parvari G, Eichen Y, Rittel D (2019) Mechanical reinforcement of methylcellulose hydrogels by rigid particle additives. Mech Mater 132:57–65. https://doi.org/10.1016/j.mechmat.2019.02.013

Sahiner N, Kaynak A, Butun S (2012) Soft hydrogels for dual use: template for metal nanoparticle synthesis and a reactor in the reduction of nitrophenols. J Non-Cryst Solids 358:758–764. https://doi.org/10.1016/j.jnoncrysol.2011.12.022

Salzano de Luna M, Ascione C, Santillo C, Verdolotti L, Lavorgna M, Buonocore GG, Castaldo R, Filippone G, Xia H, Ambrosio L (2019) Optimization of dye adsorption capacity and mechanical strength of chitosan aerogels through crosslinking strategy and graphene oxide addition. Carbohydr Polym 211:195–203. https://doi.org/10.1016/j.carbpol.2019.02.002

Saoudi O, Ghaouar N (2019) Biocatalytic characterization of free and immobilized laccase from *Trametes versicolor* in its activation zone. Int J Biol Macromol 128:681–691. https://doi.org/10.1016/j.ijbiomac.2019.01.199

Saravanan S, Vimalraj S, Anuradha D (2018) Chitosan based thermoresponsive hydrogel containing graphene oxide for bone tissue repair. Biomed Pharmacother 107:908–917. https://doi.org/10.1016/j.biopha.2018.08.072

Sato R, Kawakami T, Tokuyama H (2014) Preparation of polymeric macroporous hydrogels for the immobilization of enzymes using an emulsion-gelation method. React Funct Polym 76:8–12. https://doi.org/10.1016/j.reactfunctpolym.2014.01.001

Senthil Kumar P, Varjani SJ, Suganya S (2018) Treatment of dye wastewater using an ultrasonic aided nanoparticle stacked activated carbon: kinetic and isotherm modelling. Bioresour Technol 250:716–722. https://doi.org/10.1016/j.biortech.2017.11.097

Shah LA, Khan M, Javed R, Sayed M, Khan MS, Khan A, Ullah M (2018) Superabsorbent polymer hydrogels with good thermal and mechanical properties for removal of selected heavy metal ions. J Clean Prod 201:78–87. https://doi.org/10.1016/j.jclepro.2018.08.035

Shariatinia Z, Jalali AM (2018) Chitosan-based hydrogels: preparation, properties and applications. Int J Biol Macromol 115:194–220. https://doi.org/10.1016/j.ijbiomac.2018.04.034

Shojaeiarani J, Bajwa D, Shirzadifar A (2019) A review on cellulose nanocrystals as promising biocompounds for the synthesis of nanocomposite hydrogels. Carbohydr Polym 216:247–259. https://doi.org/10.1016/j.carbpol.2019.04.033

da Silva FR, de Moura MR, Glenn GM, Aouada FA (2018) Thermal, microstructural, and spectroscopic analysis of Ca^{2+} alginate/clay nanocomposite hydrogel beads. J Mol Liq 265:327–336. https://doi.org/10.1016/j.molliq.2018.06.005

Sirajudheen P, Meenakshi S (2019) Facile synthesis of chitosan-La^{3+}-graphite composite and its influence in photocatalytic degradation of methylene blue. Int J Biol Macromol 133:253–261. https://doi.org/10.1016/j.ijbiomac.2019.04.073

Song L, Liu FQ, Zhu CQ, Li AM (2019) Facile one-step fabrication of carboxymethyl cellulose based hydrogel for highly efficient removal of Cr(VI) under mild acidic condition. Chem Eng J 369:641–651. https://doi.org/10.1016/j.cej.2019.03.126

de Souza ÍFT, Petri DFS (2018) β-Cyclodextrin hydroxypropyl methylcellulose hydrogels for bisphenol A adsorption. J Mol Liq 266:640–648. https://doi.org/10.1016/j.molliq.2018.06.117

Su RD, Li Q, Huang RX, Zhao LW, Yue QY, Gao BY, Chen YS (2018) Biomass-based soft hydrogel for triple use: adsorbent for metal removal, template for metal nanoparticle synthesis, and a reactor for nitrophenol and methylene blue reduction. J Taiwan Inst Chem E 91:235–242. https://doi.org/10.1016/j.jtice.2018.05.007

Sun PY, Wu YH (2013) An amperometric biosensor based on human cytochrome P450 2C9 in polyacrylamide hydrogel films for bisphenol A determination. Sensors Actuators B Chem 178:113–118. https://doi.org/10.1016/j.snb.2012.12.055

Sun LY, Wang J, Yu YR, Bian FK, Zou MH, Zhao YJ (2018) Graphene oxide hydrogel particles from microfluidics for oil decontamination. J Colloid Interface Sci 528:372–378. https://doi.org/10.1016/j.jcis.2018.05.106

Sun XF, Hao Y, Cao Y, Zeng Q (2019a) Superadsorbent hydrogel based on lignin and montmorillonite for Cu(II) ions removal from aqueous solution. Int J Biol Macromol. https://doi.org/10.1016/j.ijbiomac.2019.01.058

Sun XH, Tyagi P, Agate S, Lucia L, McCord M, Pal L (2019b) Unique thermo-responsivity and tunable optical performance of poly(N-isopropylacrylamide)-cellulose nanocrystal hydrogel films. Carbohydr Polym 208:495–503. https://doi.org/10.1016/j.carbpol.2018.12.067

Tang SCN, Wang P, Yin K, Lo IMC (2010) Synthesis and application of magnetic hydrogel for Cr(VI) removal from contaminated water. Environ Eng Sci 27:947–954. https://doi.org/10.1089/ees.2010.0112

Tang SCN, Yan DYS, Lo IMC (2014) Sustainable wastewater treatment using microsized magnetic hydrogel with magnetic separation technology. Ind Eng Chem Res 53:15718–15724. https://doi.org/10.1021/ie502512h

Tang LZ, Tang F, Li M, Li LD (2018) Facile synthesis of Ag@AgCl-contained cellulose hydrogels and their application. Colloids Surf A Physicochem Eng Asp 553:618–623. https://doi.org/10.1016/j.colsurfa.2018.06.016

Thakur VK, Voicu SI (2016) Recent advances in cellulose and chitosan based membranes for water purification: a concise review. Carbohydr Polym 146:148–165. https://doi.org/10.1016/j.carbpol.2016.03.030

Thakur S, Pandey S, Arotiba OA (2016) Development of a sodium alginate-based organic/inorganic superabsorbent composite hydrogel for adsorption of methylene blue. Carbohydr Polym 153:34–46. https://doi.org/10.1016/j.carbpol.2016.06.104

Thakur S, Sharma B, Verma A, Chaudhary J, Tamulevicius S, Thakur VK (2018) Recent progress in sodium alginate based sustainable hydrogels for environmental applications. J Clean Prod 198:143–159. https://doi.org/10.1016/j.jclepro.2018.06.259

Thomas M, Naikoo GA, Sheikh MUD, Bano M, Khan F (2016) Effective photocatalytic degradation of Congo red dye using alginate/carboxymethyl cellulose/TiO_2 nanocomposite hydrogel under direct sunlight irradiation. J Photochem Photobiol A Chem 327:33–43. https://doi.org/10.1016/j.jphotochem.2016.05.005

Thompson BR, Horozov TS, Stoyanov SD, Paunov VN (2018) Hierarchically porous composites fabricated by hydrogel templating and viscous trapping techniques. Mater Des 137:384–393. https://doi.org/10.1016/j.matdes.2017.10.046

Tong DS, Fang K, Yang HY, Wang J, Zhou CH, Yu WH (2019) Efficient removal of copper ions using a hydrogel bead triggered by the cationic hectorite clay and anionic sodium alginate. Environ Sci Pollut Res Int 26:16482–16492. https://doi.org/10.1007/s11356-019-04895-8

Tran NH, Reinhard M, Gin KY (2018) Occurrence and fate of emerging contaminants in municipal wastewater treatment plants from different geographical regions—a review. Water Res 133:182–207. https://doi.org/10.1016/j.watres.2017.12.029

Ullah F, Othman MB, Javed F, Ahmad Z, Md Akil H (2015) Classification, processing and application of hydrogels: a review. Mater Sci Eng C Mater Biol Appl 57:414–433. https://doi.org/10.1016/j.msec.2015.07.053

Upama Baruah AK, Chowdhury D (2016) A sulphonated carbon dot–chitosan hybrid hydrogel nanocomposite as an efficient ion-exchange film for Ca^{2+} and Mg^{2+} removal. Nanoscale. https://doi.org/10.1039/C6NR01129B

USEPA (2019) Persistent organic pollutants: a global issue, a global response. http://www2.epa.gov/international-cooperation/persistent-organic-pollutants-global-issue-global-response. Accessed Sept 2019

Van den Broeck L, Piluso S, Soultan AH, De Volder M, Patterson J (2019) Cytocompatible carbon nanotube reinforced polyethylene glycol composite hydrogels for tissue engineering. Mater Sci Eng C Mater Biol Appl 98:1133–1144. https://doi.org/10.1016/j.msec.2019.01.020

Van Tran V, Park D, Lee YC (2018) Hydrogel applications for adsorption of contaminants in water and wastewater treatment. Environ Sci Pollut Res Int. https://doi.org/10.1007/s11356-018-2605-y

Vieira RM, Vilela PB, Becegato VA, Paulino AT (2018) Chitosan-based hydrogel and chitosan/acid-activated montmorillonite composite hydrogel for the adsorption and removal of Pb^{2+} and Ni^{2+} ions accommodated in aqueous solutions. J Environ Chem Eng 6:2713–2723. https://doi.org/10.1016/j.jece.2018.04.018

Wahid F, Yin JJ, Xue DD, Xue H, Lu YS, Zhong C, Chu LQ (2016) Synthesis and characterization of antibacterial carboxymethyl chitosan/ZnO nanocomposite hydrogels. Int J Biol Macromol 88:273–279. https://doi.org/10.1016/j.ijbiomac.2016.03.044

Wang HN, Chen L, Fang L, Li LY, Fang JJ, Lu CH, Xu ZZ (2018a) Supramolecular hydrogel hybrids having high mechanical property, photoluminescence and light-induced shape deformation capability: design, preparation and characterization. Mater Des 160:194–202. https://doi.org/10.1016/j.matdes.2018.09.018

Wang PX, Li Y, Jiang MY (2018b) Effects of the multilayer structures on Exenatide release and bioactivity in microsphere/thermosensitive hydrogel system. Colloids Surf B: Biointerfaces 171:85–93. https://doi.org/10.1016/j.colsurfb.2018.04.063

Wang T, Dai ZP, Kang JM, Fu FY, Zhang T, Wang S (2018c) A TiO_2 nanocomposite hydrogel for hydroponic plants in efficient water improvement. Mater Chem Phys 215:242–250. https://doi.org/10.1016/j.matchemphys.2018.05.042

Wang W, Zhao YL, Bai HY, Zhang TT, Ibarra-Galvan V, Song SX (2018d) Methylene blue removal from water using the hydrogel beads of poly(vinyl alcohol)-sodium alginate-chitosan-

montmorillonite. Carbohydr Polym 198:518–528. https://doi.org/10.1016/j.carbpol.2018.06.124

Wang XH, Wang YY, He SF, Hou HQ, Hao C (2018e) Ultrasonic-assisted synthesis of superabsorbent hydrogels based on sodium lignosulfonate and their adsorption properties for Ni^{2+}. Ultrason Sonochem 40: 221–229. https://doi.org/10.1016/j.ultsonch.2017.07.011

Wang Y, Du BB, Wang JY, Wang Y, Gu HN, Zhang XD (2018f) Synthesis and characterization of a high capacity ionic modified hydrogel adsorbent and its application in the removal of Cr(VI) from aqueous solution. J Environ Chem Eng 6:6881–6890. https://doi.org/10.1016/j.jece.2018.10.048

Wang H, Gong X, Guo X, Liu C, Fan YY, Zhang J, Niu B, Li W (2019a) Characterization, release, and antioxidant activity of curcumin-loaded sodium alginate/ZnO hydrogel beads. Int J Biol Macromol 121:1118–1125. https://doi.org/10.1016/j.ijbiomac.2018.10.121

Wang H, Liu ZH, Zhang J, Huang RP, Yin H, Dang Z, Wu PX, Liu Y (2019b) Insights into removal mechanisms of bisphenol A and its analogues in municipal wastewater treatment plants. Sci Total Environ 692:107–116. https://doi.org/10.1016/j.scitotenv.2019.07.134

Wang QY, Wang YX, Chen LY (2019c) A green composite hydrogel based on cellulose and clay as efficient absorbent of colored organic effluent. Carbohydr Polym 210:314–321. https://doi.org/10.1016/j.carbpol.2019.01.080

Wang W, Zhao YL, Yi H, Chen TX, Kang SC, Zhang TT, Rao F, Song SX (2019d) Pb(II) removal from water using porous hydrogel of chitosan-2D montmorillonite. Int J Biol Macromol 128:85–93. https://doi.org/10.1016/j.ijbiomac.2019.01.098

Wolf M, Paulino AT (2019) Full-factorial central composite rotational design for the immobilization of lactase in natural polysaccharide-based hydrogels and hydrolysis of lactose. Int J Biol Macromol 135: 986–997. https://doi.org/10.1016/j.ijbiomac.2019.06.032

Wu JM, Cheng X, Li YL, Yang GS (2019a) Constructing biodegradable nanochitin-contained chitosan hydrogel beads for fast and efficient removal of Cu(II) from aqueous solution. Carbohydr Polym 211: 152–160. https://doi.org/10.1016/j.carbpol.2019.01.004

Wu R, Zhang SH, Zhang Q, Liu CF, Tian GH, Lv JG (2019b) Volumetric hydrogel sensor enables visual and quantitative detection of sulfion. Sensors Actuators B Chem 282:750–755. https://doi.org/10.1016/j.snb.2018.10.117

Xia M, Kang S-M, Lee G-W, Huh YS, Park BJ (2019) The recyclability of alginate hydrogel particles used as a palladium catalyst support. J Ind Eng Chem 73:306–315. https://doi.org/10.1016/j.jiec.2019.01.042

Xing L, Sun JC, Tan HP, Yuan GL, Li JL, Jia Y, Xiong DS, Chen G, Lai JZ, Ling ZH, Chen Y, Niu XH (2019) Covalently polysaccharide-based alginate/chitosan hydrogel embedded alginate microspheres for BSA encapsulation and soft tissue engineering. Int J Biol Macromol 127:340–348. https://doi.org/10.1016/j.ijbiomac.2019.01.065

Xu YX, Yuan SP, Han JM, Lin H, Zhang XH (2017) Design and fabrication of a chitosan hydrogel with gradient structures via a step-by-step cross-linking process. Carbohydr Polym 176:195–202. https://doi.org/10.1016/j.carbpol.2017.08.032

Xu B, Wang LL, Liu YW, Zhu HL, Wang Q (2018) Preparation of high strength and transparent nanocomposite hydrogels using alumina nanoparticles as cross-linking agents. Mater Lett 228:104–107. https://doi.org/10.1016/j.matlet.2018.05.135

Yang JH, Li ZK, Zhu HJ (2017) Adsorption and photocatalytic degradation of sulfamethoxazole by a novel composite hydrogel with visible light irradiation. Appl Catal B Environ 217:603–614. https://doi.org/10.1016/j.apcatb.2017.06.029

Yang T, Li Q, Wen WX, Hu L, He WW, Liu HZ (2018a) Cadmium sulfide quantum dots/poly(acrylic acid-co-acrylic amide) composite hydrogel synthesized by gamma irradiation. Radiat Phys Chem 145: 130–134. https://doi.org/10.1016/j.radphyschem.2017.10.012

Yang XZ, Zhou TZ, Ren BZ, Hursthouse A, Zhang YZ (2018b) Removal of Mn (II) by sodium alginate/graphene oxide composite double-network hydrogel beads from aqueous solutions. Sci Rep 8: 10717–10732. https://doi.org/10.1038/s41598-018-29133-y

Yang F, Fan X, Zhang M, Wang C, Zhao WF, Zhao CS (2019a) A template-hatched method towards poly(acrylic acid) hydrogel spheres with ultrahigh ion exchange capacity and robust adsorption of environmental toxins. J Ind Eng Chem 69:422–431. https://doi.org/10.1016/j.jiec.2018.10.004

Yang XJ, Zhang P, Li P, Li ZT, Xia W, Zhang HY, Di ZG, Wang ML, Zhang HQ, Niu QJ (2019b) Layered double hydroxide/polyacrylamide nanocomposite hydrogels: green preparation, rheology and application in methyl orange removal from aqueous solution. J Mol Liq 280:128–134. https://doi.org/10.1016/j.molliq.2019.02.033

Yao TJ, Jia WJ, Tong X, Feng Y, Qi Y, Zhang X, Wu J (2018) One-step preparation of nanobeads-based polypyrrole hydrogel by a reactive-template method and their applications in adsorption and catalysis. J Colloid Interface Sci 527:214–221. https://doi.org/10.1016/j.jcis.2018.05.052

Yin S, Ma ZF (2019) "Smart" sensing interface for the improvement of electrochemical immunosensor based on enzyme-Fenton reaction triggered destruction of Fe^{3+} cross-linked alginate hydrogel. Sensors Actuators B Chem 281:857–863. https://doi.org/10.1016/j.snb.2018.11.030

Yu L, Liu XK, Yuan WC, Brown LJ, Wang DY (2015) Confined flocculation of ionic pollutants by poly(L-dopa)-based polyelectrolyte complexes in hydrogel beads for three-dimensional, quantitative, efficient water decontamination. Langmuir 31:6351–6366. https://doi.org/10.1021/acs.langmuir.5b01084

Yu C, Tang XZ, Liu SW, Yang YL, Shen XC, Gao CC (2018a) Laponite crosslinked starch/polyvinyl alcohol hydrogels by freezing/thawing process and studying their cadmium ion absorption. Int J Biol Macromol 117:1–6. https://doi.org/10.1016/j.ijbiomac.2018.05.159

Yu KH, Wang D, Wang QM (2018b) Tough and self-healable nanocomposite hydrogels for repeatable water treatment. Polymers (Basel). https://doi.org/10.3390/polym10080880

Yu F, Cui TR, Yang CF, Dai XH, Ma J (2019) *k*-Carrageenan/sodium alginate double-network hydrogel with enhanced mechanical properties, anti-swelling, and adsorption capacity. Chemosphere. https://doi.org/10.1016/j.chemosphere.2019.124417

Yue YY, Wang XH, Han JQ, Yu L, Chen JQ, Wu QL, Jiang JC (2019a) Effects of nanocellulose on sodium alginate/polyacrylamide hydrogel: mechanical properties and adsorption-desorption capacities. Carbohydr Polym 206:289–301. https://doi.org/10.1016/j.carbpol.2018.10.105

Yue YY, Wang XH, Wu QL, Han JQ, Jiang JC (2019b) Assembly of polyacrylamide-sodium alginate-based organic-inorganic hydrogel with mechanical and adsorption properties. Polymers (Basel). https://doi.org/10.3390/polym11081239

Zareie C, Bahramian AR, Sefti MV, Salehi MB (2019) Network-gel strength relationship and performance improvement of polyacrylamide hydrogel using nano-silica; with regards to application in oil wells conditions. J Mol Liq 278:512–520. https://doi.org/10.1016/j.molliq.2019.01.089

Zazakowny K, Lewandowska-Lancucka J, Mastalska-Poplawska J, Kaminski K, Kusior A, Radecka M, Nowakowska M (2016) Biopolymeric hydrogels-nanostructured TiO_2 hybrid materials as potential injectable scaffolds for bone regeneration. Colloids Surf B: Biointerfaces 148:607–614. https://doi.org/10.1016/j.colsurfb.2016.09.031

Zhang QW, Wang Y, Mateescu A, Sergelen K, Kibrom A, Jonas U, Wei T, Dostalek J (2013) Biosensor based on hydrogel optical waveguide spectroscopy for the detection of 17β-estradiol. Talanta 104: 149–154. https://doi.org/10.1016/j.talanta.2012.11.017

Zhang JS, Yao TJ, Guan CC, Zhang NX, Zhang H, Zhang X, Wu J (2017) One-pot preparation of ternary reduced graphene oxide nanosheets/Fe_2O_3/polypyrrole hydrogels as efficient Fenton catalysts. J Colloid Interface Sci 505:130–138. https://doi.org/10.1016/j.jcis.2017.05.101

Zhang HY, Fei X, Tian J, Li Y, Zhi H, Wang K, Xu LQ, Wang Y (2018a) Synthesis and continuous catalytic application of alkaline protease nanoflowers–PVA composite hydrogel. Catal Commun 116:5–9. https://doi.org/10.1016/j.catcom.2018.07.015

Zhang W, Cheng W, Ziemann E, Be'er A, Lu XL, Elimelech M, Bernstein R (2018b) Functionalization of ultrafiltration membrane with polyampholyte hydrogel and graphene oxide to achieve dual antifouling and antibacterial properties. J Membr Sci 565:293–302. https://doi.org/10.1016/j.memsci.2018.08.017

Zhang CD, Li HD, Yu QZ, Jia L, Wan LY (2019a) Poly(aspartic acid) electrospun nanofiber hydrogel membrane-based reusable colorimetric sensor for Cu(II) and Fe(III) detection. ACS Omega 4:14633–14639. https://doi.org/10.1021/acsomega.9b02109

Zhang H, Omer AM, Hu ZH, Yang LY, Ji C, Ouyang XK (2019b) Fabrication of magnetic bentonite/carboxymethyl chitosan/sodium alginate hydrogel beads for Cu (II) adsorption. Int J Biol Macromol 135:490–500. https://doi.org/10.1016/j.ijbiomac.2019.05.185

Zhang Q, Hu XM, Wu MY, Wang MM, Zhao YY, Li TT (2019c) Synthesis and performance characterization of poly(vinyl alcohol)-xanthan gum composite hydrogel. React Funct Polym 136:34–43. https://doi.org/10.1016/j.reactfunctpolym.2019.01.002

Zhao LZ, Zhou CH, Wang J, Tong DS, Yua WH, Wang H (2015) Recent advances in clay mineral-containing nanocomposite hydrogels. Soft Matter 11:9229–9246. https://doi.org/10.1039/C5SM01277E

Zhao L, Deng JH, Sun PZ, Liu JS, Ji Y, Nakada N, Qiao Z, Tanaka H, Yang YK (2018a) Nanomaterials for treating emerging contaminants in water by adsorption and photocatalysis: systematic review and bibliometric analysis. Sci Total Environ 627:1253–1263. https://doi.org/10.1016/j.scitotenv.2018.02.006

Zhao PP, Yu F, Wang RY, Ma Y, Wu YQ (2018b) Sodium alginate/graphene oxide hydrogel beads as permeable reactive barrier material for the remediation of ciprofloxacin-contaminated groundwater. Chemosphere 200:612–620. https://doi.org/10.1016/j.chemosphere.2018.02.157

Zheng YA, Wang AQ (2015) Superadsorbent with three-dimensional networks: from bulk hydrogel to granular hydrogel. Eur Polym J 72:661–686. https://doi.org/10.1016/j.eurpolymj.2015.02.031

Zhou JH, Hao BZ, Wang LB, Ma JZ, Cheng WJ (2017) Preparation and characterization of nano-TiO_2/chitosan/poly(N-isopropylacrylamide) composite hydrogel and its application for removal of ionic dyes. Sep Purif Technol 176:193–199. https://doi.org/10.1016/j.seppur.2016.11.069

Zhou AJ, Chen W, Liao L, Xie PC, Zhang TC, Wu XM, Feng XN (2019) Comparative adsorption of emerging contaminants in water by functional designed magnetic poly(N-isopropylacrylamide)/chitosan hydrogels. Sci Total Environ 671:377–387. https://doi.org/10.1016/j.scitotenv.2019.03.183

Zhu HJ, Li ZK, Yang JH (2018) A novel composite hydrogel for adsorption and photocatalytic degradation of bisphenol A by visible light irradiation. Chem Eng J 334:1679–1690. https://doi.org/10.1016/j.cej.2017.11.148

Zhuang YT, Jiang R, Wu DF, Yu YL, Wang JH (2019) Selenocarrageenan-inspired hybrid graphene hydrogel as recyclable adsorbent for efficient scavenging of dyes and Hg^{2+} in water environment. J Colloid Interface Sci 540:572–578. https://doi.org/10.1016/j.jcis.2019.01.060